

Rotational and angular distributions from photodissociations.

III. Effects of dynamic axis switching in linear triatomic molecules

Michael D. Morse^{a)} and Karl F. Freed^{b)}

The James Franck Institute and The Department of Chemistry, The University of Chicago, Chicago, Illinois 60637

(Received 29 February 1980; accepted 27 March 1980)

An analysis is presented of the effects of dynamic axis switching on the three-dimensional quantum mechanical theory of photodissociations of linear triatomic molecules. The dynamic axis switching phenomenon arises from the fact that there are small deviations of the orientation of the diatomic fragment axis from that of the equilibrium triatomic molecule axis in the initially bound state of the molecule. While these deviations vanish on the average, the dynamic axis switching is shown under certain circumstances to alter significantly the calculated rotational, orbital angular momentum and angular distributions from the results of the previous work in which these small deviations are ignored. The dynamic axis switching is demonstrated to be important for determining the proper partitioning of the triatomic initial state rotational angular momentum (J) into nascent diatomic rotational angular momentum and orbital angular momentum of the atom about the diatom. Thus, the dynamic axis switching effect vanishes for $J = 0$. The effects of this dynamical axis switching transformation are shown to be particularly important for dissociations involving heavy atomic fragments, with lighter atomic fragments giving a smaller effect. The correspondence is established between these quantum mechanical results and those obtained classically. Illustrative calculations are provided of the rotation-bending factor contribution to rotational energy and state resolved angular distributions in HCN and ICN photodissociation. Bending vibrations influence the angular distributions such that a state averaged distribution produces a preferred off-axis recoil direction which can be related to the mean square bending amplitude in the initial bound state.

I. INTRODUCTION

One of the primary processes in a wide variety of photochemical reactions is photodissociation. Despite its great importance, the detailed description of the photodissociation of an isolated molecule has been adequately treated only for the case of diatomic molecules where the problem is relatively straightforward if only a single repulsive potential curve enters.¹⁻⁵ The few degrees of freedom present in a diatomic molecule permit the direct application of conservation laws, simplifying any calculations considerably.

Consider, on the other hand, the photodissociation of a polyatomic molecule. As the molecule fragments, the normal modes of vibration undergo drastic changes, and new rotational degrees of freedom appear. Furthermore, the fragments may have completely different geometries than they had in the bound state of the molecule. Reorganization of the electronic structure of the molecule may even result in the formation of chemical bonds between atoms that were not directly bonded to each other in the initial state of the molecule (as occurs in the photodissociation⁶⁻⁹ of formaldehyde into CO plus H₂). These major changes in molecular structure make polyatomic photodissociations both intrinsically more interesting than those of diatomics and more difficult to treat theoretically as well.

The additional degrees of freedom that are present in polyatomic molecules prompt us to ask how the excess energy, that is released in the dissociation, is partitioned among these degrees of freedom. This question

is rarely of much importance in the dissociations of diatomic molecules, since the only degrees of freedom relevant to the energy partitioning are the electronic excitations of the fragment atoms and the translational motion of the atoms as they separate. For diatomic dissociations involving only a single repulsive potential curve, only one electronic state is obtained for each atom, and the translational energy is rigorously determined by energy conservation. For dissociations producing diatomic or polyatomic fragments, however, there are additional rotational and vibrational degrees of freedom that can absorb some of the energy that is released in the dissociation, and the distributions of energy within these degrees of freedom are of considerable interest.

In part, this work is motivated by the substantial recent technological advances that have made it possible for experimentalists to carry out close approximations to state-selected and state-analyzed experiments. Notable examples of these experiments include Ashfold and Simons's work on the vacuum ultraviolet photolysis of cyano compounds XCN¹⁰⁻¹⁵ and Baronavski and McDonald's laser induced fluorescence studies of photofragments produced from the near ultraviolet photolysis of ICN¹⁶ and HN₃.¹⁷ More recently, two-photon excitation has been used to monitor the product NO rovibronic distributions in the photodissociation of CF₃NO.¹⁸ In addition, Dagdigian and Zare's recent measurements of state-to-state angular distributions in chemical reactions¹⁹⁻²¹ shows that the application of these techniques to the study of state-to-state photofragment angular distributions is quite feasible.

The past 10 or 15 years have thus witnessed a proliferation of experimental methods which provide much

^{a)}Fannie and John Hertz Foundation Fellow.

^{b)}Research supported, in part, by NSF Grant CHE 77-24652.

more detailed data about photodissociations than were available in the past. With such quantities of detailed experimental data becoming available, it is important to develop a theoretical understanding of molecular photodissociation processes for chemical species larger than simple diatomic molecules. The simplest case of a polyatomic molecular photodissociation is, of course, the linear triatomic molecule, and this must be understood thoroughly before proceeding to larger polyatomic molecules.

The theory of the photodissociation of linear triatomic molecules has been studied by many researchers in various approximations. In the earliest works a collinear model was adopted, using bond oscillators rather than the correct normal modes.²²⁻²⁵ In subsequent work the correct stretching normal modes were incorporated, but all three atoms were still constrained to lie on a non-rotating line.²⁶⁻³¹ Few treatments have appeared which have attempted to include bending and rotational motions. Florida and Rice included these motions in their study of HCCl photodissociation,³² but did not use the proper normal modes of the molecule. In previous works, we have shown how the bending and rotational motions may be properly incorporated, thus permitting calculations of state-to-state photofragment rotational³³⁻³⁵ and angular³⁶ distributions.

In the description of the motions of a bound state of a linear triatomic molecule, it is most convenient to refer to a body fixed axis system rotating with the equilibrium principal axes of inertia of the molecule. In the description of the motions of the dissociated state of the molecule, on the other hand, the most natural coordinate system uses the axis of the diatomic molecule and the atom-diatom vector as the relevant coordinates. On average, when the molecule is undergoing bending vibrations, the diatomic axis is the same as the equilibrium axis of the bound triatomic state. Thus, it seems to be a good approximation to take the angles describing these two axes as identical. This is the approximation we have invoked in our previous works.³³⁻³⁶ In this paper, we lift this approximation and explicitly consider the effects of a dynamical axis switching transformation which correctly transforms from the set of angles describing the equilibrium triatomic molecule axis to the angles of the diatomic fragment. The dynamic axis switching effects become small or vanish in the limits of low triatomic initial angular momentum and of the dissociation of a light atomic fragment. It is shown, however, that this transformation is essential to properly describe the photodissociations of linear triatomics producing heavy atomic fragments, as in the case of ICN.

Section II gives the theory of the photodissociation of a linear triatomic molecule, and the derivation of the axis-switching transformation is explicitly presented. In Sec. III, the rotational-bending contribution to photofragment rotational and orbital angular momentum distributions are presented, using HCN and ICN as illustrative examples. These distributions are compared to the classical limiting cases. In Sec. IV, we derive state-to-state photofragment angular distributions. High energy limiting calculations for HCN and ICN are compared

to the distributions obtained through semiclassical theories. Bending vibrations in HCN are shown to produce state averaged angular distributions with apparent off-axis recoil. Section V discusses our major conclusions, and the appendices contain the relevant mathematical details.

II. PHOTODISSOCIATION OF A LINEAR TRIATOMIC MOLECULE

In the case of direct photodissociations, involving weak electromagnetic fields, the decay rate for transitions from state i to state f is given accurately by the usual "golden rule" expression^{27,28}

$$\Gamma_{fi} = \left| \int \Psi_f(\mathbf{Q}) V(\mathbf{Q}) \Psi_i(\mathbf{Q}) d\mathbf{Q} \right|^2 \quad (\text{II. 1})$$

in the Born-Oppenheimer approximation, where $V(\mathbf{Q})$ is the $i \rightarrow f$ state electronic transition moment of the matter-radiation interaction Hamiltonian. In Eq. (II. 1), $\Psi_f(\mathbf{Q})$ represents the exact nuclear wave function on the dissociative potential energy surface, which asymptotically is described by the quantum numbers f and is normalized to 2π times a delta function in energy. $\Psi_i(\mathbf{Q})$ describes the exact nuclear wave function on the initial potential energy surface.

The golden rule may be similarly applied to predissociations if the perturbation V inducing the dissociation is sufficiently weak and the predissociating states are well separated in energy (nonoverlapping). In this case $V(\mathbf{Q})$ is the off-diagonal electronic matrix element of the perturbation inducing the $i \rightarrow f$ dissociation, and $\Psi_i(\mathbf{Q})$ is the nuclear wave function of the initially prepared predissociating state.^{27,28}

For dissociations from a well-defined initially prepared predissociating state, there is no preferred direction in space and $V(\mathbf{Q})$ is zero-rank tensor (scalar coupling). In this case, the only spatial anisotropy that may arise is due to the method of preparation of the predissociating state. On the other hand, for direct photodissociation the direction of polarization of the absorbed photon determines a preferred direction in space. The electric dipole approximation is usually a sufficient approximation in this event, resulting in a first-rank tensorial coupling $V(\mathbf{Q})$ and the familiar dipole selection rules for total angular momentum J . These limit the angular momentum change upon absorption ΔJ to 0, ± 1 , so $V(\mathbf{Q})$ may be approximated as a zero-rank tensor so long as the rotational distributions calculated for J , $J \pm 1$ are very similar. The relevant tensorial algebra, retaining the full dipole treatment, is presented in Appendix A, where this expectation is shown to be valid.

For the moment, then, let us treat $V(\mathbf{Q})$ as a zero-rank tensor for simplicity. Furthermore, for allowed transitions, we may invoke the Condon approximation that $V(\mathbf{Q})$ is a slowly varying function of \mathbf{Q} in the region of nuclear coordinates important in the evaluation of the integral, so that Eq. (II. 1) becomes

$$\Gamma_{fi} = \left| \bar{V} \int \Psi_f(\mathbf{Q}) \Psi_i(\mathbf{Q}) d\mathbf{Q} \right|^2 \quad (\text{II. 2})$$

The Condon approximation also applies in the case of

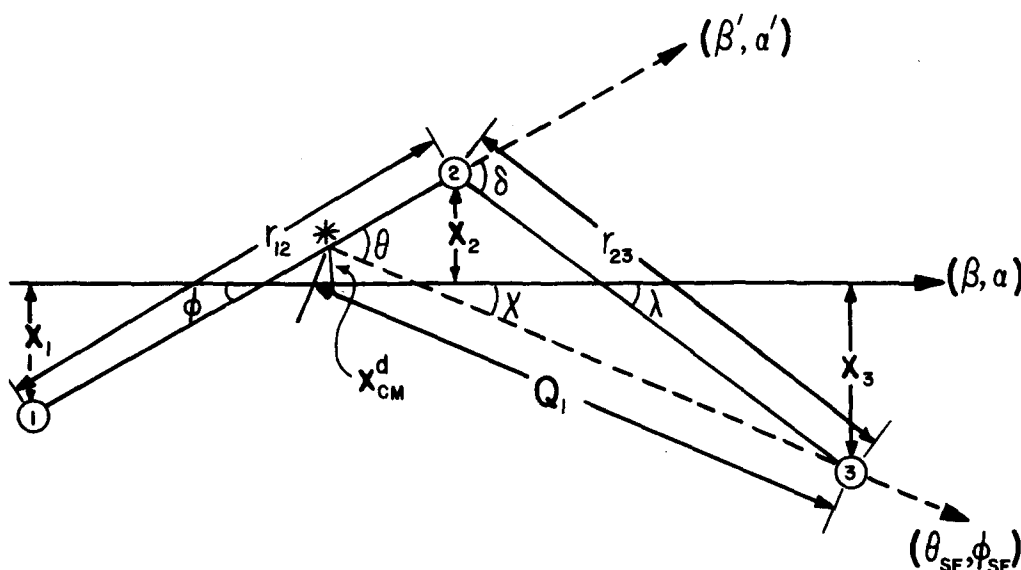


FIG. 1. The coordinates used in the theory, (β, α) , (β', α') , and $(\theta_{\text{SF}}, \phi_{\text{SF}})$ denote the spherical polar angles of the equilibrium principal axis of inertia, the diatomic axis, and the atom-diatom vector, respectively, measured in the space-fixed frame. The angles δ , θ , ϕ , χ , and λ are all measure angles between vectors in the plane of the instantaneously bent molecule, as indicated in the figure, and are all positive numbers. The center of mass of atoms 1 and 2 is indicated by an asterisk, and the displacements of the atoms from their equilibrium positions are denoted by x_i . Bond 2-3 breaks in the photodissociation process.

predissociation by spin-orbit coupling, where $V(\mathbf{Q})$ is usually taken to be a slowly varying function of \mathbf{Q} .³⁷ With minor changes a similar approximation may be made for cases of predissociation by the failure of the Born-Oppenheimer approximation, or cases of vibronically induced direct photodissociation.^{27,28} The incorporation of corrections due to the \mathbf{Q} dependence of $V(\mathbf{Q})$ has been discussed previously, and similar considerations may be applied here.^{34,37}

A. Basis wave functions

The appropriate choice of coordinate system for the initially bound state of the triatomic molecule consists of the normal (or local) mode coordinates of the molecule. The initial state wave function is then given as a product of wave functions for these modes. For the linear triatomic molecule these include two stretching vibrational coordinates Q_1 and Q_2 , and the angle δ , which gives the angle of the bend, measured relative to a linear configuration. The angles (β, α) are the Euler angles specifying the orientation of the equilibrium axis of inertia of the triatomic molecule, and γ is an azimuthal angle about this axis which defines the plane of the instantaneously bent molecule. With this coordinate system (see Fig. 1), we may express the basis rotational-vibrational wave function as

$$\Psi_i(\mathbf{Q}) = \left(\frac{2J+1}{8\pi^2} \right)^{1/2} D_{Mk}^{J*}(\alpha, \beta, \gamma) \psi_{n_1}(Q_1) \psi_{n_2}(Q_2) \psi_\nu^k(\delta), \quad (\text{II. 3})$$

where a harmonic zeroth order potential has been invoked for the bending and stretching vibrations. Thus, $\psi_{n_1}(Q_1)$ and $\psi_{n_2}(Q_2)$ are the familiar harmonic-oscillator wave functions³⁸

$$\psi_n(Q) = 2^{-n/2} (n!)^{-1/2} \left(\frac{\mu\omega}{\hbar\pi} \right)^{1/4} \times \exp\left(-\frac{\mu\omega}{2\hbar} Q^2\right) H_n\left(\sqrt{\frac{\mu\omega}{\hbar}} Q\right), \quad (\text{II. 4})$$

and $\psi_\nu^k(\delta)$ is a two-dimensional isotropic harmonic-oscillator function with vibrational angular momentum k along the axis³⁹

$$\psi_\nu^k(\delta) = \kappa \left[\frac{2 \binom{\nu - |k|}{2}!}{\binom{\nu + |k|}{2}!} \right]^{1/2} (\kappa\delta)^{|k|} \times \exp\left(-\frac{\kappa^2\delta^2}{2}\right) L_{\binom{\nu - |k|}{2}}^{|k|}(\kappa^2\delta^2), \quad (\text{II. 5})$$

where

$$\kappa = \left[\frac{(\gamma_{12}^0)^2 (\gamma_{23}^0)^2}{\frac{(\gamma_{12}^0)^2}{m_3} + \frac{(\gamma_{23}^0)^2}{m_1} + \frac{(\gamma_{12}^0 + \gamma_{23}^0)^2}{m_2}} \frac{\omega_{\text{bend}}}{\hbar} \right]^{1/2}. \quad (\text{II. 6})$$

Anharmonicities and vibration-rotation couplings may be treated by forming linear combinations of basis functions of the form of Eq. (II. 3). Since each of the individual contributions may be treated term by term as described below, we continue with Eq. (II. 3) for notational simplicity.

The final state wave function is described in terms of the coordinates appropriate in the asymptotic region of separated fragments. Here the angles β' and α' denote the polar and azimuthal angles, respectively, of the diatomic axis, while θ_{SF} and ϕ_{SF} denote the corresponding angles of the vector from the diatom center of mass to the third atom. In the asymptotic limit, the relative motion of the fragments separates from the diatomic vibration, so the appropriate coordinates are Q'_1 and Q'_2 , with Q'_1 the distance from atom 3 to the diatom center of mass and Q'_2 the vibrational coordinate for the diatomic stretching. Thus, the appropriate asymptotic wave function has the form

$$\Psi_f(\mathbf{Q}) = \sum_{\mu m} \langle \hat{J} \hat{M} | l j \mu m \rangle \times Y_{l\mu}(\theta_{\text{SF}}, \phi_{\text{SF}}) Y_{j m}(\beta', \alpha') \psi_n(Q'_2) \psi_{E l}(Q'_1), \quad (\text{II. 7})$$

with $\langle \hat{J} \hat{M} | l j \mu m \rangle$ a vector coupling coefficient to provide eigenstates of total angular momentum \hat{J} and space-fixed z projection \hat{M} .

In the case of symmetrical molecules, such as CO_2 , the asymptotic wave function Ψ_f cannot be of the form of

Eq. (II. 7), since either end atom may break off. In this case, asymptotically the wave function Ψ_f must go to a linear combination of terms like Eq. (II. 7), with separate amplitudes for each of the two possible fragmentations.

Equation (II. 7) is the exact nuclear wave function for a separable potential, and gives no inelastic scattering on the unbound potential surface. For a realistic treatment of the dissociation, linear combinations of terms of this type must be used, with the $\psi_{E_i}(Q_i')$ functions determined by the solution of a set of coupled equations, or approximations to these coupled equations must be introduced to account for the scattering. Band, Freed, and Kouri⁴⁰ have recently shown how the photodissociation problem with a nonseparable final state potential surface may be treated by the solution of a set of close-coupled *inhomogeneous* differential equations. The inhomogeneous terms in these equations act as driving terms which provide sources of flux, and involve precisely the same Franck-Condon integrals which arise when Eq. (II. 7) is used in the golden rule (II. 1). Thus, the evaluation of Franck-Condon factors, involving separable wave functions such as Eq. (II. 7), is an important step in the economical solution of the general coupled equations for the photodissociation problem with nonseparable final potential surfaces, and we concentrate on this Franck-Condon aspect of the problem here.

B. Relations between molecular axes

For a linear molecule in its equilibrium configuration, the principal axis of the molecule coincides with the axis of the resulting diatomic fragment, and no rotation or axis-switching transformation⁴¹ is required to transform the angles (β, α) to (β', α') , provided the molecule is constrained to remain at its equilibrium angle ($\delta = 0$). However, as the molecule bends, these axes depart from coincidence, and we define ϕ to be the angle between them (see Fig. 1).

In our previous works³³⁻³⁶ we have taken $\phi = 0$, so the axis systems appropriate to the initial and final states coincide, and $(\beta, \alpha) \equiv (\beta', \alpha')$. If (β', α') is averaged over the bending vibrations of the molecule, this identity is obtained on the average. However, at any given instantaneous displacement from linearity the axis systems appropriate to the two states differ slightly. As bending vibrations are generally small in amplitude, and ϕ is always less than δ , the previous neglect in differences between (β, α) and (β', α') seems to be a reasonable approximation. This paper examines the effects of the dynamical axis-switching transformation⁴¹ which relates (β, α) to (β', α') as a function of δ , and shows how this approximation can introduce grave errors in certain cases.

For small bends, ϕ is proportional to δ , with the result

$$\phi = \rho \delta . \quad (\text{II. 8})$$

The constant ρ may be determined by considering the signed displacements of the atoms from the equilibrium axis x_i (as indicated in Fig. 1) and noting the center-of-mass constraint

$$\sum_i m_i x_i = 0 = (m_1 + m_2 + m_3)x_{c.m.} . \quad (\text{II. 9})$$

An additional constraint is that the angular momentum be conserved as the molecule bends. The familiar Eckart conditions define the rotating coordinate system as the one for which the angular momentum vanishes when all the atoms are in their equilibrium condition

$$\sum_i m_i (\mathbf{r}_i^0 - \mathbf{r}_{c.m.}^0) \times (\dot{\mathbf{r}}_i - \dot{\mathbf{r}}_{c.m.}) = 0 \quad (\text{II. 10})$$

with \mathbf{r}^0 the equilibrium positions. Since Eq. (II. 9) fixes the center of mass, we also have

$$\sum_i m_i \dot{x}_i = 0 . \quad (\text{II. 11})$$

Considering the bending to occur in the x - z plane in the rotating coordinate system, the y component of Eq. (II. 10) yields

$$\begin{aligned} L_y &= \sum_i m_i (z_i^0 - z_{c.m.}^0) (\dot{x}_i - \dot{x}_{c.m.}) = 0 \\ &= \sum_i m_i z_i^0 \dot{x}_i - z_{c.m.} \left(\sum_i m_i \dot{x}_i \right) \\ &\quad - \dot{x}_{c.m.} \left(\sum_i m_i z_i^0 \right) + z_{c.m.} \dot{x}_{c.m.} \left(\sum_i m_i \right) = 0 . \end{aligned} \quad (\text{II. 12})$$

Relations (II. 9) and (II. 11) cause all terms except the first to vanish. For convenience, let $z_2 = 0$, so Eq. (II. 12) yields

$$m_1 r_{12}^0 \dot{x}_1 - m_3 r_{23}^0 \dot{x}_3 = 0 , \quad (\text{II. 13})$$

which upon integration gives the constraint

$$m_1 r_{12}^0 x_1 - m_3 r_{23}^0 x_3 = 0 . \quad (\text{II. 14})$$

(The equilibrium case sets the integration constant to zero.)

From Fig. 1 we deduce that

$$\phi = \sin^{-1} \frac{x_2 - x_1}{r_{12}} , \quad (\text{II. 15})$$

$$\delta = \phi + \lambda = \sin^{-1} \frac{x_2 - x_1}{r_{12}} + \sin^{-1} \frac{x_2 - x_3}{r_{23}} . \quad (\text{II. 16})$$

For small bends, these reduce to

$$\phi = \frac{x_2 - x_1}{r_{12}} , \quad (\text{II. 17})$$

$$\delta = \frac{x_2 - x_1}{r_{12}} + \frac{x_2 - x_3}{r_{23}} . \quad (\text{II. 18})$$

Elimination of x_1 , x_2 , x_3 from Eqs. (II. 9), (II. 14), (II. 17), and (II. 18) results in expression (II. 8), where ρ is given by

$$\rho = \frac{m_3 r_{23}^0 [(m_1 + m_2) r_{23}^0 + m_1 r_{12}^0]}{m_3 (m_1 + m_2) r_{23}^0 + 2 m_1 m_3 r_{12}^0 r_{23}^0 + m_1 (m_2 + m_3) r_{12}^0} . \quad (\text{II. 19})$$

[Note that we have approximated r_{12} and r_{23} in Eqs. (II. 17) and (II. 18) by their equilibrium values.]

Similarly, we note that for small bends, θ is also proportional to δ :

$$\theta = \eta \delta \quad (\text{II. 20})$$

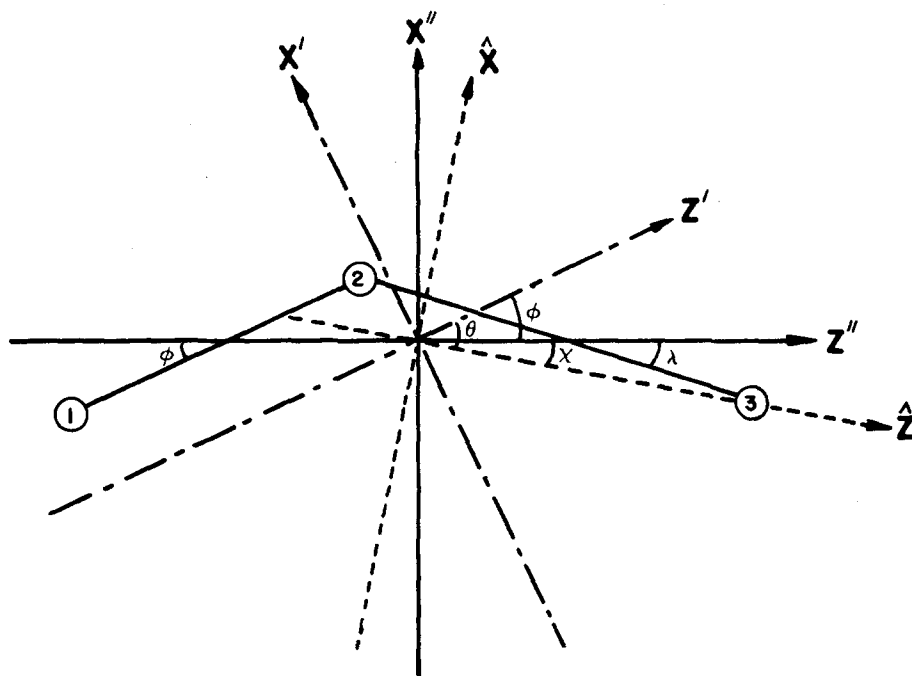


FIG. 2. Body-fixed axis systems. Rotating with the molecule are the three coordinate systems (x', y', z') , (x'', y'', z'') , and $(\hat{x}, \hat{y}, \hat{z})$. These coordinate systems have the z axis along the diatomic axis, the triatomic equilibrium principal axis of inertia, and the atom to diatom center-of-mass vector, respectively, with the x coordinate of atom 3 negative in the (x', y', z') and (x'', y'', z'') coordinate systems. The x coordinate of atom 1 is negative in the $(\hat{x}, \hat{y}, \hat{z})$ coordinate system. The angles θ , ϕ , and χ relate the three coordinate systems to each other.

as follows: From Fig. 1, it is evident that

$$\theta = \phi + \chi. \quad (\text{II. 21})$$

Defining $x_{\text{c.m.}}^d = (m_1 x_1 + m_2 x_2)/(m_1 + m_2)$, we note that χ is given by

$$\chi = \sin^{-1} \frac{x_{\text{c.m.}}^d - x_3}{Q_1'}, \quad (\text{II. 22})$$

where by the law of cosines it follows that

$$Q_1' = \sqrt{r_{23}^2 + \left(\frac{m_1 r_{12}}{m_1 + m_2}\right)^2 - 2 \frac{m_1 r_{12} r_{23}}{m_1 + m_2} \cos \delta}. \quad (\text{II. 23})$$

Thus, for small bends, we find

$$\theta = \frac{x_2 - x_1}{r_{12}} + \frac{x_{\text{c.m.}}^d - x_3}{r_{23} + \frac{m_1 r_{12}}{m_1 + m_2} + o(\delta)}. \quad (\text{II. 24})$$

Again, we may eliminate x_1 , x_2 , and x_3 from Eqs. (II. 9), (II. 14), (II. 18), and (II. 24) to obtain Eq. (II. 20) with η given as

$$\eta = \frac{(m_1 + m_2)r_{23}^0}{(m_1 + m_2)r_{23}^0 + m_1 r_{12}^0}, \quad (\text{II. 25})$$

where once again we have approximated r_{12} and r_{23} in Eqs. (II. 18) and (II. 24) by their equilibrium values.

C. Transformations between different coordinate systems

In order to transform the wave functions (II. 3) and (II. 7) into the same coordinate system, relations between (α, β, γ) , (α', β') , $(\theta_{\text{SF}}, \phi_{\text{SF}})$, and δ must be introduced. This requires considerable care, since mistakes are easy to make at this stage. We define the following coordinate systems (see Fig. 2):

$\{x, y, z\}$ is a space-fixed frame;

$\{x', y', z'\}$ is body fixed, with the diatomic vector

pointing in the z' direction, with the molecule in the $y' = 0$ plane, and atom 3 with $x_3' \leq 0$;

$\{x'', y'', z''\}$ is body fixed, with the instantaneous principal axis of inertia along the z'' axis, the molecule in the $y'' = 0$ plane, and atom 3 with $x_3'' \leq 0$;

$\{\hat{x}, \hat{y}, \hat{z}\}$ is body fixed, with the diatom center of mass to atom vector pointing along the \hat{z} axis, the molecule in the $\hat{y} = 0$ plane, with $\hat{x}_1 \leq 0$.

These axis systems are related by the following rotation operations:

$$R(\alpha, \beta, \gamma)\{x, y, z\} = \{x'', y'', z''\}, \quad (\text{II. 26})$$

$$R(\alpha', \beta', \gamma')\{x, y, z\} = \{x', y', z'\}, \quad (\text{II. 27})$$

$$R(\phi_{\text{SF}}, \theta_{\text{SF}}, \gamma_{\text{SF}})\{x, y, z\} = \{\hat{x}, \hat{y}, \hat{z}\}, \quad (\text{II. 28})$$

$$R(0, \phi, 0)\{x'', y'', z''\} = \{x', y', z'\}, \quad (\text{II. 29})$$

$$R(0, \theta, 0)\{\hat{x}, \hat{y}, \hat{z}\} = \{x', y', z'\}. \quad (\text{II. 30})$$

Here we use the notation $R(\alpha, \beta, \gamma)\{xyz\}$ to denote the rotation of the $\{xyz\}$ coordinate system by the Euler angles (α, β, γ) , as defined by Rose.⁴²

Noting that Eqs. (II. 26)–(II. 30) yield

$$R(0, \phi, 0)R(\alpha, \beta, \gamma)\{x, y, z\} = R(\alpha', \beta', \gamma')\{x, y, z\}, \quad (\text{II. 31})$$

$$R(0, \theta, 0)R(\phi_{\text{SF}}, \theta_{\text{SF}}, \gamma_{\text{SF}})\{x, y, z\} = R(\alpha', \beta', \gamma')\{x, y, z\}, \quad (\text{II. 32})$$

enables us to relate these various angles through the addition theorem of rotation matrices,⁴² obtaining

$$D_{mm'}^j(\alpha', \beta', \gamma') = \sum_{m''} D_{mm''}^j(\alpha, \beta, \gamma) D_{m''m'}^j(0, \phi, 0) \quad (\text{II. 33})$$

and

$$D_{mm'}^j(\alpha', \beta', \gamma') = \sum_{m''} D_{mm''}^j(\phi_{SF}, \theta_{SF}, \gamma_{SF}) D_{m''m}^j(0, \theta, 0). \quad (\text{II. 34})$$

These equations may be solved for (α, β, γ) and $(\phi_{SF}, \theta_{SF}, \gamma_{SF})$ in terms of $(\alpha', \beta', \gamma')$, ϕ , and θ to obtain

$$D_{mm'}^j(\alpha, \beta, \gamma) = \sum_{m''} D_{mm''}^j(\alpha', \beta', \gamma') D_{m''m}^{j*}(0, \phi, 0), \quad (\text{II. 35})$$

$$D_{mm'}^j(\phi_{SF}, \theta_{SF}, \gamma_{SF}) = \sum_{m''} D_{mm''}^j(\alpha', \beta', \gamma') D_{m''m}^{j*}(0, \theta, 0). \quad (\text{II. 36})$$

Both of these relations are crucial for the evaluation of the Franck-Condon factor, as detailed in Appendix A, where we obtain for $\langle f | i \rangle$ the two equivalent convenient forms

$$\begin{aligned} \langle f | i \rangle &= \left[\frac{(2j+1)(2l+1)}{2(2J+1)} \right]^{1/2} \delta_{M\hat{M}} \delta_{J\hat{J}} \sum_{m'} \langle Jm' | ljm'0 \rangle \\ &\times \langle d_{0m}^j(\theta) \psi_n(Q_2) \psi_{E1}(Q_1) | d_{km}^j(\phi) \psi_{n_1}(Q_1) \psi_{n_2}(Q_2) \psi_{\nu}^k(\delta) \rangle, \end{aligned} \quad (\text{II. 37a})$$

$$\begin{aligned} \langle f | i \rangle &= \left[\frac{(2j+1)(2l+1)}{2(2J+1)} \right]^{1/2} \delta_{M\hat{M}} \delta_{J\hat{J}} \sum_{m'} \langle Jm' | ljm'0 \rangle \\ &\times \langle d_{m'0}^j(\theta) \psi_n(Q_2) \psi_{E1}(Q_1) | d_{m'k}^j(\theta - \phi) \psi_{n_1}(Q_1) \psi_{n_2}(Q_2) \psi_{\nu}^k(\delta) \rangle. \end{aligned} \quad (\text{II. 37b})$$

D. Simplification of Franck-Condon factors

The difficulty in evaluating the expressions (II. 37) arises because the three-dimensional integrals involve functions which are expressed in both of the essentially different coordinate systems associated with the bound and dissociative surfaces. A transformation relating the variables of the initially bound state of the system (Q_1, Q_2, δ) to the variables of the final state wave function (Q_1', Q_2', θ) must be found, so that the integrals may be evaluated in a single coordinate system. When this transformation is introduced, it is found that the integrals (II. 37) are nonseparable, providing an essential difficulty in the theory.

For collinear dissociations, a transformation between (Q_1, Q_2) and (Q_1', Q_2') has been previously derived^{27,28}, now in the full three-dimensional description it becomes weakly dependent on δ . Similarly, Eq. (II. 20) gives the transformation between θ and δ , and had we not approximated r_{12} and r_{23} in Eqs. (II. 18) and (II. 24) by their equilibrium values this transformation would be dependent on the stretching coordinates (r_{12}, r_{23}) [or alternatively on (Q_1, Q_2) or (Q_1', Q_2')].

In the photodissociation of a triatomic molecule, which is initially bound, Franck-Condon factors derive most of their amplitude from a very localized region in space. Thus, only a small range of Q_1 , Q_2 , and δ contribute to the integral. Essentially, this is a result of the small amplitudes of vibration of the molecule in its initially bound state. Thus, although the relation between θ and δ does depend on the stretching coordinates, this dependence is extremely slight because the root-mean square displacements Δr_{12} and Δr_{23} are much smaller than r_{12}^0 and r_{23}^0 . For all practical purposes it is sufficient to re-

gard η as a constant, with the values of r_{12} and r_{23} in Eq. (II. 25) determined either by their equilibrium values in the bound state of the triatomic, or more accurately by use of the Q -centroid method.^{34,37} The treatment of the corrections due to these variations follows the procedure given previously.³⁴

Similarly, the transformation between (Q_1, Q_2) and (Q_1', Q_2') is weakly dependent on δ , but this variation may be ignored since δ is constrained to small values and the first correction is of order δ^2 . These arguments can, of course, be made more precise, by separating the integrand into portions that are weakly dependent on various variables, and expanding these parts in Taylor series as has been described in previous papers.³⁴ Such a method then permits an analysis of the importance of nonseparability on the rotational distributions in the photofragments.

For the illustrative calculations presented here, such a treatment is not warranted. Here we adopt harmonic oscillator wave functions in the various normal modes and thereby already introduce a small oscillation approximation in the initial state of the molecule. In ignoring these weak dependences of the initial-final state coordinate transformation, we are simply invoking the same small oscillation approximation again. Of course, in the case of molecules undergoing large amplitude vibrations, this could be an important source of error (as in, for example, photodissociations of van der Waals complexes like HeI_2), and the fuller theory along the lines of Appendix B of Ref. 34 can then be used.

As has been demonstrated previously,³⁴ the evaluation of matrix elements of wave functions in different coordinate systems requires, in addition to the wave functions themselves, an extra factor of the square root of the Jacobian. Using the matrix C' to transform (Q_1', Q_2') to (Q_1, Q_2) ^{27,28} and the approximations discussed above, we obtain from Eq. (II. 37a)

$$\langle f | i \rangle = |\det C'|^{1/2} F_{E1} G(\nu, k, l, j, J) \delta_{J\hat{J}} \delta_{M\hat{M}}, \quad (\text{II. 38})$$

where the stretches-translational factor is

$$F_{E1} = \int_{-\infty}^{+\infty} dQ_1' \int_{-\infty}^{+\infty} dQ_2' \psi_n^*(Q_2') \psi_{E1}^*(Q_1') \psi_{n_1}(Q_1) \psi_{n_2}(Q_2) \quad (\text{II. 39})$$

and the rotation-bending factor is

$$\begin{aligned} G(\nu, k, l, j, J) &= \left[\frac{(2j+1)(2l+1)}{2(2J+1)} \right]^{1/2} \sum_{m'} \langle Jm' | ljm'0 \rangle \eta \\ &\times \int_0^{\infty} d\delta \delta d_{0m}^j(\eta\delta) d_{km}^j(\rho\delta) \psi_{\nu}^k(\delta). \end{aligned} \quad (\text{II. 40})$$

An equivalent expression, quite similar in form, is readily obtained from Eq. (II. 37b). The integral (II. 39) for the stretches and relative motions is of the same form as arises in collinear models of dissociation processes, and it may be evaluated by the methods given by Band and Freed.^{27,28} It should be emphasized that their method applies to larger polyatomic molecules in the collinear model; it is the severe complications associated with the description of the rotations and bends that limits us here to triatomic molecules.

Hougen and Watson⁴¹ have shown that for small θ ,

$d_{KK}^J(\theta) \propto J_{|K-K'|}(J\theta)$, with $J_{|K-K'|}$ a Bessel function. By examination of the differential equation for $d_{KK}^J(\theta)$, and by making small angle approximations $\cos\theta = 1$, $\sin\theta = \theta$, we obtain Bessel's equation. We evaluate the proportionality factor that relates $d_{KK}^J(\theta)$ to its Bessel approximation by matching the first nonvanishing derivative at $\theta = 0$, and this gives

$$d_{KK}^J(\theta) = (J + \frac{1}{2})^{-1} J_{|K-K'|} \left[\frac{(J+K')!(J-K)!}{(J-K')!(J+K)!} \right]^{1/2} J_{|K-K'|}((J + \frac{1}{2})\theta), \quad \text{for } K' \geq K, \quad (\text{II. 41})$$

$$d_{KK}^J(\theta) = (-1)^{K-K'} (J + \frac{1}{2})^{-1} J_{|K-K'|} \left[\frac{(J-K')!(J+K)!}{(J+K')!(J-K)!} \right]^{1/2} \times J_{|K-K'|}((J + \frac{1}{2})\theta), \quad \text{for } K \geq K'. \quad (\text{II. 42})$$

Using this small angle Bessel approximation, the small angle formulas (II. 8) and (II. 20) for ϕ and θ , respectively, a standard integral [Ref. 43, (6. 6333. 2)], and recursion relations for Bessel functions and Laguerre polynomials, analytic results for the rotation-bending Franck-Condon factor (II. 40) have been obtained (see Appendix B). The corrections due to the dependences of the initial-final state coordinate transformations which have been ignored here can be evaluated by previously described methods.^{34,37}

III. PHOTOFRAGMENT ROTATIONAL AND ORBITAL ANGULAR MOMENTUM DISTRIBUTIONS

Equation (II. 38) shows that $\langle f|i \rangle$ is a product of a vibration-translation factor F_{E1} and a rotational-bending factor G . When Eq. (II. 38) is squared to obtain transition probabilities and a summation is performed over the irrelevant quantum numbers (generally l) we obtain a convolution of $|F_{E1}|^2$ and $|G|^2$. The factor $|F_{E1}|^2$ contains the constraints of energy conservation, and therefore depends implicitly on J and j . The constraints of angular momentum conservation, on the other hand, are contained in $|G|^2$. Because the probability distributions are a convolution of $|F_{E1}|^2$ and $|G|^2$, it makes sense to study them independently. As $|F_{E1}|^2$ has already been extensively studied,^{27,28,44} we focus attention on the rotational-bending factor $|G|^2$ and the effects of angular momentum conservation in this section.

Expressions (II. 38)-(II. 40) are particularly useful in the determination of the probability distribution of orbital angular momentum l . Restricting attention to only the $|G|^2$ contribution, the summation of final j states may be analytically performed, giving

$$P_J(l) = (l + \frac{1}{2})\eta^2 \sum_m \left[\int_0^\infty d\delta \delta d_{0m}^l(\eta\delta) d_{km}^J(\rho\delta) \psi_\nu^k(\delta) \right]^2. \quad (\text{III. 1})$$

The actual distribution in l requires the retention of $|F_{E1}|^2$ which is a function of j through energy conservation constraints. The approximation (III. 1) is useful to illustrate the basic structure of $|G|^2$ that is independent of the stretching and translational degrees of freedom. For a complete description it is necessary to perform a convolution involving $|G|^2$ and $|F_{E1}|^2$. Often the dependence of $|F_{E1}|^2$ on j and l is weak enough for Eq. (III.1) to be an accurate first approximation. Expressions analogous to (II. 38)-(II. 40), derived from Eq. (II. 37b),

are more useful for obtaining the fragment diatomic rotational distribution $P_J(i)$ since in this case dropping the l dependence of F_{E1} enables the summation over final orbital angular momentum to be analytically performed, giving the approximation from $|G|^2$ alone:

$$P_J(j) = (j + \frac{1}{2})\eta^2 \sum_m \left[\int_0^\infty d\delta \delta d_{0m}^j(\eta\delta) d_{km}^J((\eta - \rho)\delta) \psi_\nu^k(\delta) \right]^2. \quad (\text{III. 2})$$

Analytic expressions for Eqs. (III. 1) and (III. 2) are given in Appendix B.

The similarity of expressions (III. 1) and (III. 2) is quite striking, and indicates that, apart from the omitted energy conservation constraints, the angular momenta j and l enter the theory on equal footing, with the precise distributions depending on the molecular geometry and masses, through η and ρ .

It is well known that Bessel functions of high orders have small amplitudes near the origin. When the Bessel approximations (II. 41) and (II. 42) are used in Eq. (III. 2), we obtain integrands involving $J_{|k-m|}((j + \frac{1}{2})\eta\delta) \times J_{|k-m|}((J + \frac{1}{2})(\eta - \rho)\delta)$. Since the integrand is constrained to small values of δ by the $\psi_\nu^k(\delta)$ term, we expect only small values of $|m|$ and $|k-m|$ to have important contributions to the sum. Of course, for large j and J , larger values of $|m|$ and $|k-m|$ begin contributing, but these terms are only of significance when $(j + \frac{1}{2})\eta/\kappa \geq |m|$ and $(J + \frac{1}{2})(\eta - \rho)/\kappa \geq |k-m|$. These conditions involve the range of the bending vibration given by $1/\kappa$ and the fact that the first peak of $J_m(x)$ falls at $x > m$. Since $\eta, \rho < 1$ and κ is typically 4-7, these contributions are appreciable only for $j > 6|m|$, $J > 6|k-m|$. Since we are generally interested in only low-lying excitations of the bending mode, k is usually small, and under these conditions the J and j dependent prefactors in the Bessel approximation are close to unity [e.g., for $J = 30$, $k = 2$, $k' = 7$ the prefactor of Eq. (II. 41) is 0.941]. Thus, the only significant J dependence in Eqs. (III. 1) and (III. 2) occurs in a Bessel function $J_{|k-m|}((J + \frac{1}{2})\rho\delta)$ for Eq. (III. 1) and $J_{|k-m|}((J + \frac{1}{2})(\eta - \rho)\delta)$ for Eq. (III. 2). Consequently, we expect the orbital angular momentum distribution $P_J(l)$ given by Eq. (III. 1) to be nearly identical to the diatomic rotational distribution $P_{J^*}(j)$, which is obtained at a value of $J^* = J[\rho/(\eta - \rho)]$. Indeed, this is precisely what is found in explicit numerical calculations using Eqs. (III. 1) and (III. 2) (see Figs. 3-12).

A. Distributions arising from nonrotating initial states

When $J = 0$, $k = 0$ the only value of m contributing to Eqs. (III. 1) and (III. 2) is $m = 0$. This simplifies the expressions considerably and permits us to obtain simple analytical results in these cases. However, for excited bending modes with vibrational angular momentum, the lowest possible value of J is given by $J = k$, and the integrals of Eq. (III. 1) and (III. 2) do not simplify. However, using the Bessel approximation introduces the Bessel functions $J_{|k-m|}((J + \frac{1}{2})\rho\delta)$ and $J_{|k-m|}((J + \frac{1}{2})(\eta - \rho)\delta)$ into the integrands. To consider the nonrotating limit of states with vibrational angular momentum, we set $J = k$. Since $\rho, \eta - \rho < 1$ and since the range of δ is $1/\kappa$, the only values of m that contribute significantly are

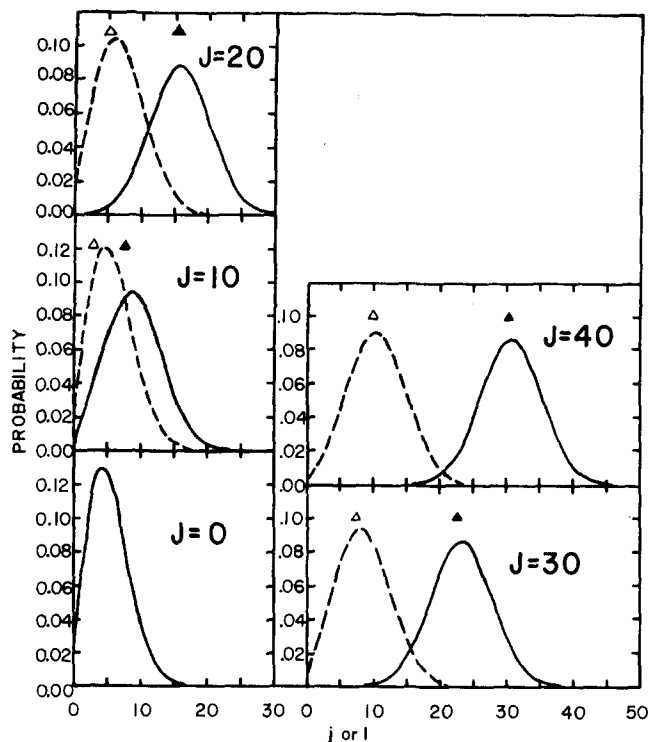


FIG. 3. Angular momentum distributions for HCN photodissociation ($\rho=0.15268$, $\eta=0.63178$, $\kappa=4.1763$) from the $|G|^2$ term alone. Solid lines indicate quantum probability distributions for diatomic CN rotational angular momentum j . The classical value is indicated by \blacktriangle . Dashed lines indicate quantum probability distributions for orbital angular momentum l . The classical value is indicated by \triangle . These results are for HCN initially in its $\nu=0$, $k=0$ bending state, for various values of total angular momentum J .

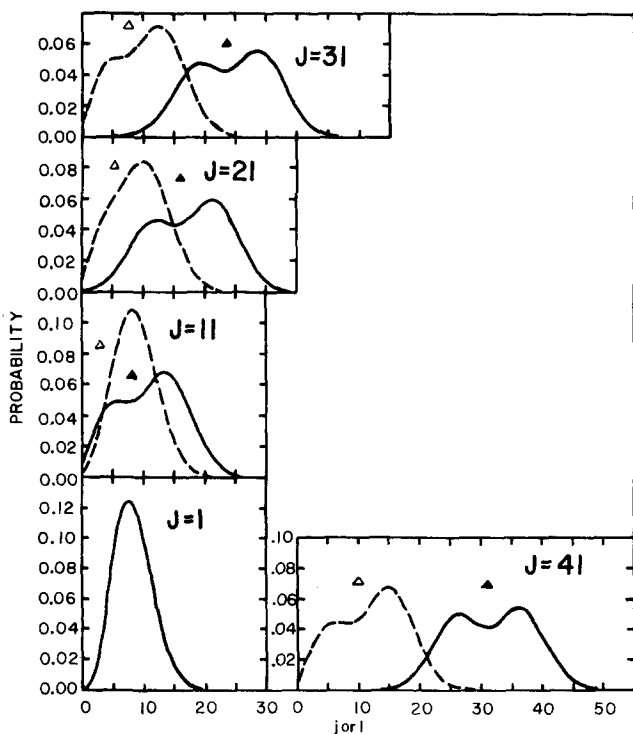


FIG. 4. Same as Fig. 3 but for HCN initially in its $\nu=1$, $k=1$ bending state. Note that this calculation utilizes only the $k=+1$ state, which is not one of the parity eigenfunctions (linear combinations of $k=\pm 1$).

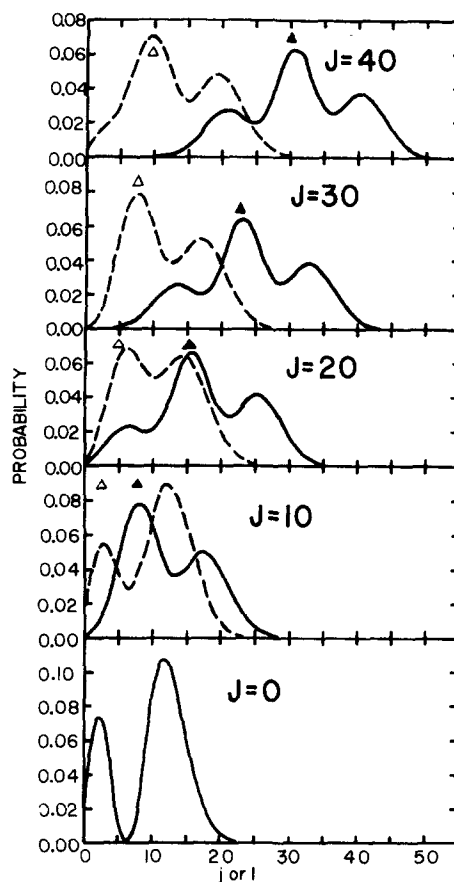


FIG. 5. Same as Fig. 3 but for HCN initially in its $\nu=2$, $k=0$ bending state.

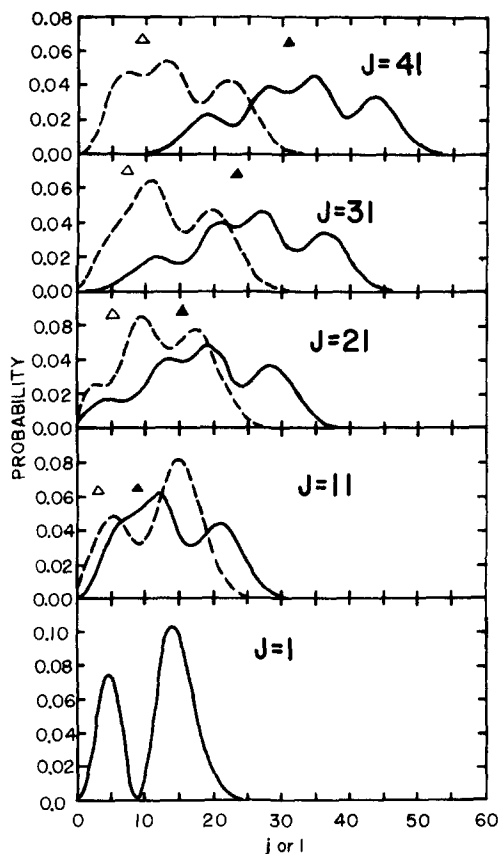


FIG. 6. Same as Fig. 3 but for HCN initially in its $\nu=3$, $k=1$ bending state. See note on Fig. 4.

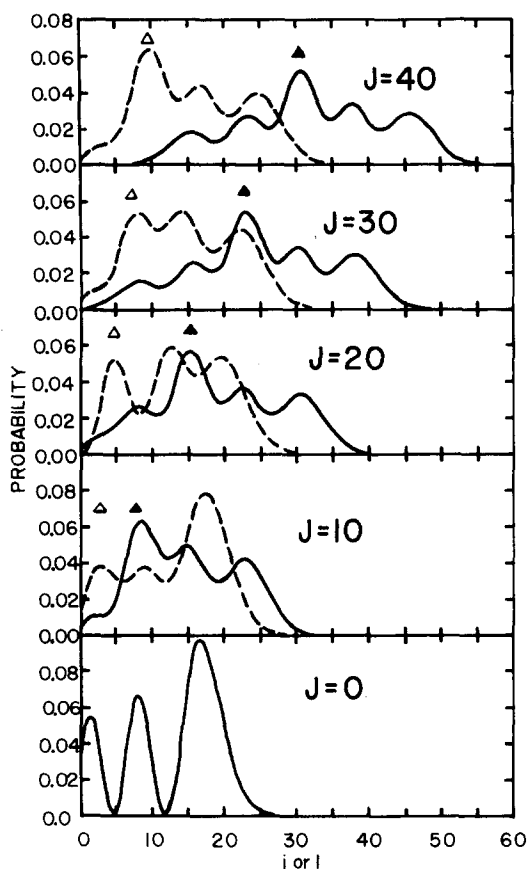


FIG. 7. Same as Fig. 3 but for HCN initially in its $\nu=4$, $k=0$ bending state.

those for which $J_{1k-m}((k+\frac{1}{2})\rho/\kappa)$ or $J_{1k-m}((k+\frac{1}{2})(\eta-\rho)/\kappa)$ is appreciable. For $k \leq 2$, ρ and $\eta-\rho$ less than 1, and $\kappa \sim 6$, we should consider $J_{1k-m}(x)$ where x is less than 0.4. A glance at tabulated values of Bessel functions shows that the contributions are dominated by the term $m=k$, for which we approximate $J_{1k-m}((k+\frac{1}{2})\rho\delta) = J_{1k-m}((k+\frac{1}{2})(\eta-\rho)\delta) = 1$. This enables us to obtain simple analytic approximations for Eqs. (III.1) and (III.2) in the nonrotating limit.

Under this limit expressions (III.1) and (III.2) reduce to the same form, namely,

$$P_{J_{\text{min}}}(l) = (l + \frac{1}{2})\eta^2 \left| \int_0^\infty d\delta \delta d_{0k}^l(\eta\delta) \psi_\nu^k(\delta) \right|^2. \quad (\text{III. 3})$$

This arises by omitting all terms in Eq. (III.1) except $m=k$, and setting $d_{kk}^k(\rho\delta) = 1$ (small angle approximation). Adopting the Bessel approximation and utilizing a standard integral [Ref. 43, (7.421.4)] we obtain

$$P_{J_{\text{min}}}(l) = (2l+1) \left(\frac{\eta}{\kappa}\right)^{2+2k} \frac{(l+k)! \left(\frac{\nu-k}{2}\right)!}{(l-k)! \left(\frac{\nu+k}{2}\right)!} \times \left[L_{\nu-k/2}^k \left(\frac{\eta^2(l+\frac{1}{2})^2}{\kappa^2} \right) \right]^2 \exp \left[-\frac{\eta^2(l+\frac{1}{2})^2}{\kappa^2} \right]. \quad (\text{III. 4})$$

The analogous nonrotating limit for $P_{J_{\text{min}}}(j)$ is given by replacing l by j in Eq. (III.4).

These distributions for the case of nonrotating initial states are precisely the same as the distributions we obtained in earlier work,³⁴ in which the effects of dynamical axis switching are neglected. All the conclusions, reached in our earlier work³⁴ for nonrotating initial states, are thus unchanged. For example, we still calculate that for nonrotating initial states, the average fragment rotational energy $\langle E_j \rangle$ and root-mean square deviation from this average $\sigma(E_j) = (\langle E_j^2 \rangle - \langle E_j \rangle^2)^{1/2}$ are

$$\langle E_j \rangle = \frac{\kappa^2 B}{\eta^2} (\nu + 1), \quad (\text{III. 5})$$

$$\sigma(E_j) = \frac{\kappa^2 B}{\eta^2} \left(\frac{\nu^2}{2} + \nu + 1 \right)^{1/2}. \quad (\text{III. 6})$$

Thus, large amplitude bending vibrations, where κ is small, partition relatively little energy into rotations, while stiff bending modes, with correspondingly larger values of κ , partition more energy into fragment rotation. This is readily explained³⁴ in terms of the Heisenberg uncertainty principle.

Another important aspect of the nonrotating limit is the result that the rotational distribution $P_{J=0}(j)$ for the ground bending state is precisely a Boltzmann distribution, with an "effective temperature" of $T = B\kappa^2/k\eta^2$, where B is the diatomic rotational constant and k is

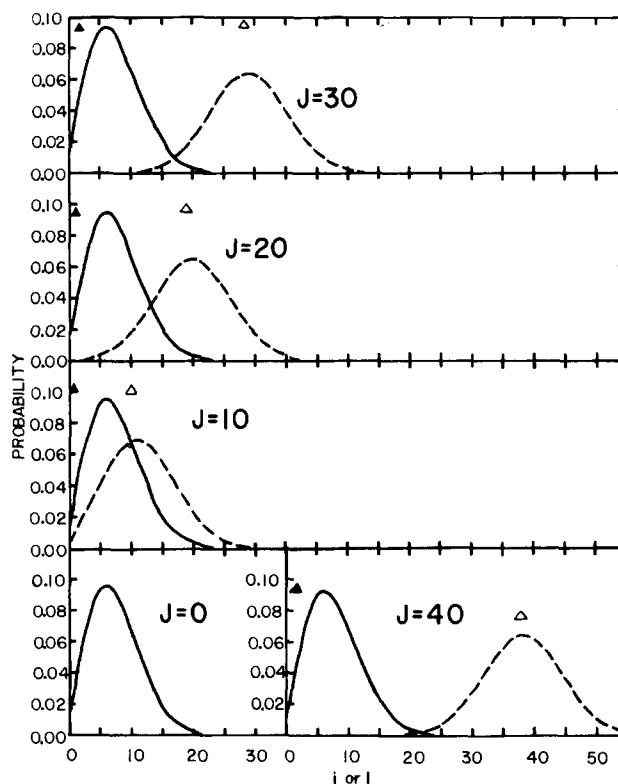


FIG. 8. Angular momentum distributions for ICN photodissociation ($\rho=0.71953$, $\eta=0.76172$, $\kappa=6.80599$) from the $|G|^2$ term alone. Solid lines indicate quantum probability distributions for diatomic CN rotational angular momentum j . The classical value is indicated by \blacktriangle . Dashed lines give quantum probability distributions for orbital angular momentum l . The classical value is indicated by \triangle . These results are for ICN initially in its $\nu=0$ $k=0$ bending state, for various values of total angular momentum J .

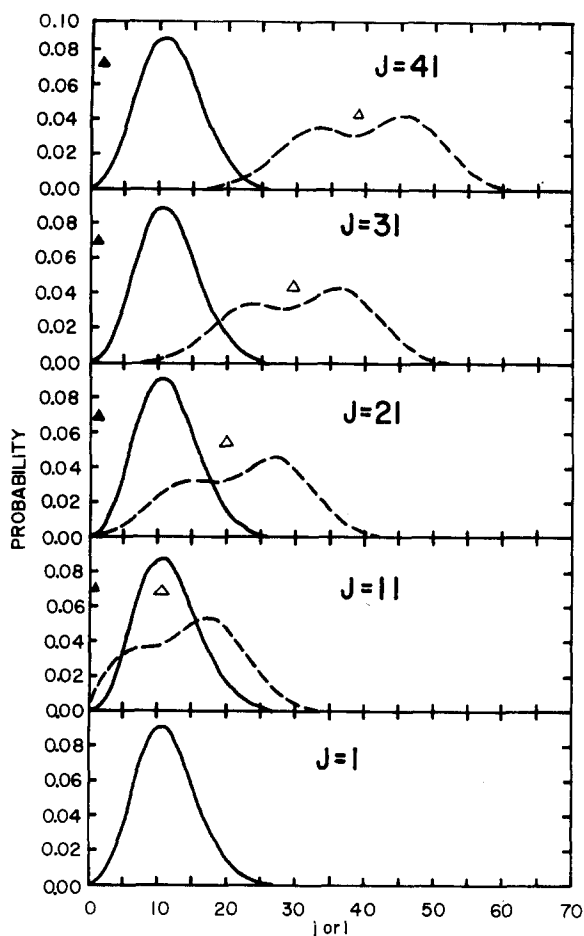


FIG. 9. Same as Fig. 8, but for ICN initially in its $\nu=1$, $k=1$ bending state. See note on Fig. 4.

Boltzmann's constant. This distribution is calculated *without any thermal averaging* over initial states, and *without any assumptions of energy randomization* during the photodissociation process. It arises solely from the Franck-Condon factors which govern the process, and would be changed slightly if an anharmonic initial state wave function were used. Furthermore, even in the photodissociations of nonrotating but vibrationally excited molecules, the calculated rotational distributions exhibit the same Boltzmann form, but are multiplied by a polynomial function of j . Thus, it is not surprising that photodissociation experiments on rotationally cold molecules should give near-Boltzmann fragment rotational distributions.

B. Distributions for rapidly rotating initial states (large J limit)

The phenomenon of dynamical axis switching may have a considerable effect on the photofragment rotational and orbital angular momentum distributions for molecules which are rotating, however. In order to assess the effects of molecular rotation on the orbital angular momentum and rotational distributions, we consider the limit of large initial angular momentum. As shown in Appendix B, the distributions $P_j(l)$ and $P_j(j)$ given by Eqs. (III.1) and (III.2) are very complicated functions, in general, involving modified Bessel functions and

Gaussians of the form

$$\exp \left[- \frac{(l + \frac{1}{2})^2 \eta^2 + (J + \frac{1}{2})^2 \rho^2}{\kappa^2} \right] \left\{ I_{\nu} \left[\frac{(l + \frac{1}{2})(J + \frac{1}{2}) \rho \eta}{\kappa^2} \right] \right\}^2. \quad (\text{III. 7})$$

If J is sufficiently large, we may take the asymptotic limit of the modified Bessel function, which is given as [Ref. 43, (8.451.5)]

$$I_{\nu}(z) \propto \frac{\exp(z)}{\sqrt{2\pi z}}. \quad (\text{III. 8})$$

Thus, for sufficiently large J , the distribution $P_j(l)$ is governed by a factor of the form

$$\exp \left\{ - \frac{1}{\kappa^2} [(l + \frac{1}{2})\eta - (J + \frac{1}{2})\rho]^2 \right\}, \quad (\text{III. 9})$$

multiplied by a complicated function that is less sharply peaked. In the large J limit, we expect the distributions $P_j(l)$ to be centered about $l^* = (J + \frac{1}{2})(\rho/\eta) - \frac{1}{2}$.

These results are indeed obtained in explicit numerical calculations using the explicit expressions of Appendix B for Eqs. (III.1) and (III.2). In fact, these conclusions correspond to the classical limit for sudden axial recoil photodissociation from the equilibrium configuration. We consider a rigid, linear triatomic molecule, rotating with angular momentum $(J + \frac{1}{2})\hbar$. This specifies an angular velocity ω given by $\omega = (J + \frac{1}{2})\hbar/I_3$, where I_3 is the triatomic moment of inertia. If we sud-

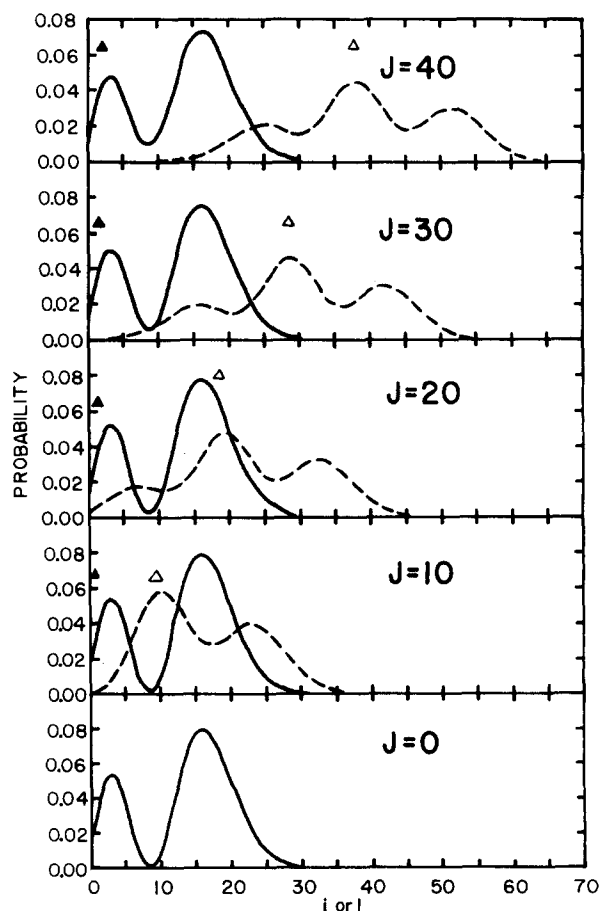


FIG. 10. Same as Fig. 8, but for ICN initially in its $\nu=2$, $k=0$ bending state.

denly break the bond connecting atoms 2 and 3, and allow the atoms to depart without change in their momentum, we obtain diatomic rotational angular momentum $(j + \frac{1}{2})\hbar = \omega I_2$, where I_2 is the moment of inertia of the diatomic molecule. Thus, the classical result is

$$j^* = (J + \frac{1}{2}) \frac{I_2}{I_3} - \frac{1}{2}. \quad (\text{III. 10})$$

Similarly, the classical value of orbital angular momentum works out to be

$$l^* = (J + \frac{1}{2}) \frac{I_3 - I_2}{I_3} - \frac{1}{2}. \quad (\text{III. 11})$$

With ρ and η determined through the small angle approximation as Eqs. (II. 19) and (II. 25), it is found that $I_2/I_3 = (\eta - \rho)/\eta$ and $(I_3 - I_2)/I_3 = \rho/\eta$, so in the limit of high J , the classical results are obtained.

C. Numerical calculations

Figures 3–12 present plots of the approximate distributions $P_j(l)$ and $P_j(j)$ based on the $|G|^2$ factor alone for various initial bending states ν^k for HCN and ICN at a series of values of total angular momentum J . The classical predictions for j and l are also indicated, and the approach toward the classical limit is evident as J increases.

In the case of photodissociations from excited bending

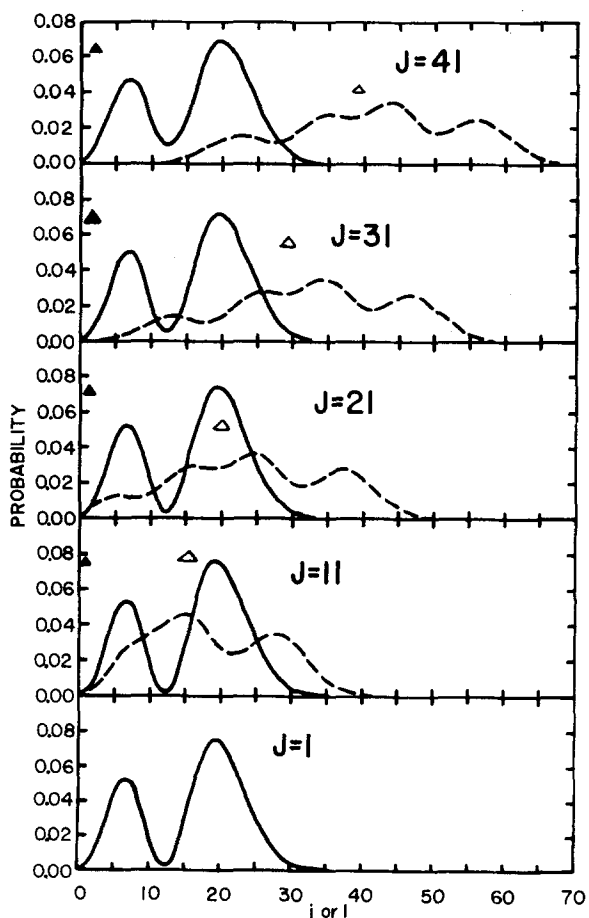


FIG. 11. Same as Fig. 8, but for ICN initially in its $\nu=3$, $k=1$ bending state. See note on Fig. 4.

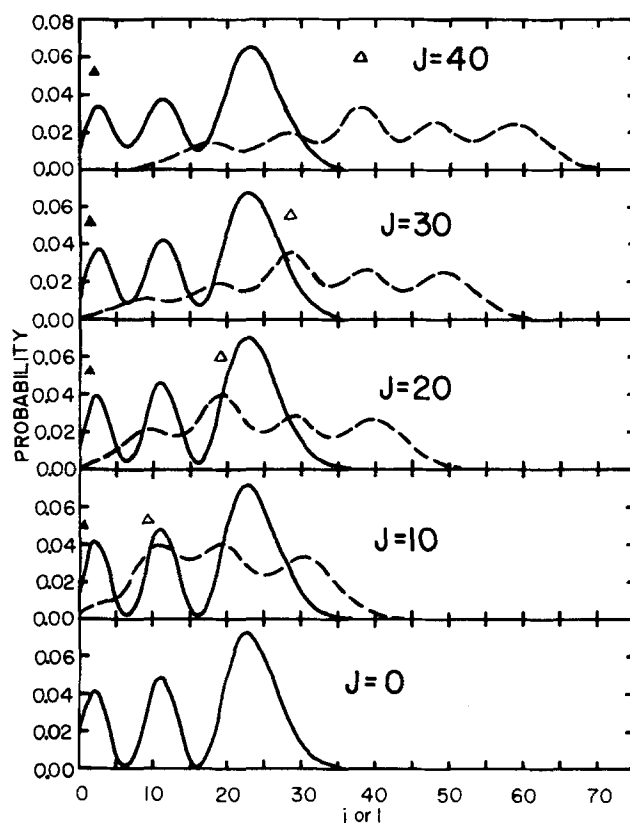


FIG. 12. Same as Fig. 8, but for ICN initially in its $\nu=4$, $k=0$ bending state.

states, considerable structure is displayed in the rotational distributions. This arises from the presence of nodes in the bending wave function. Such structure may be difficult to measure experimentally, since it may be washed out by the variation of F_{E1}^2 with j and l , by the effects of thermal averaging over the total angular momentum J in the initial bound state of the triatomic molecule, and by the averaging due to final state interactions. There are specific cases, however, such as ICN, where the dependence of the rotational distribution on the initial J state of the molecule is so slight that thermal averaging over J does not affect the rotational distributions noticeably. Such molecules, having extremely heavy atomic fragments, are appropriate examples to study if the predicted nodal structure in the rotational distributions, arising from excited bending modes, is to be experimentally verified. Even in these cases, however, the effects of the variation of $|F_{E1}|^2$ with j and l and of final state interactions may remove much of the structure in the predicted $|G|^2$ factor distributions. It is the effects of the final state interactions which are most uncertain at this point, since the variation of the $|F_{E1}|^2$ factor may readily be incorporated using the methods developed in previous works for its evaluation.^{27,28,44}

IV. PHOTOFRAGMENT ANGULAR DISTRIBUTIONS

Experimental methods for the measurement of photofragment angular distributions were developed in the late 1960's by Bersohn and co-workers,^{45–53} and refined by Wilson^{54–57} and Diesen.⁵⁸ It is expected that further refinements in experimental technique will provide con-

siderably more detailed information about photofragment angular distributions in the near future. Specifically, it is hoped that angularly resolved laser-induced fluorescence studies will enable the determination of state-to-state photofragment angular distributions. This technique has successfully been applied to measure state-analyzed angular distributions in chemical reactions by Zare and Dagdigan.¹⁹⁻²¹ With this possibility in mind, we calculate the state-to-state photofragment angular distributions for linear triatomic molecule photodissociations, using many of the results of Sec. II.

A. Theory

For weak radiation fields, the transition amplitude from initial molecular state i to final fragment state f is given in dipole approximation (as shown in Appendix A) by

$$\langle f | V | i \rangle = \sum_{qM''} (-1)^q e_q \langle \phi_f(\mathbf{x}, \mathbf{Q}) | \sum_j x_{jM''} | \phi_i(\mathbf{x}, \mathbf{Q}) \rangle, \quad (IV.1)$$

$$\langle \Psi_f(\mathbf{Q}) | D_{qM''}^{1*}(\alpha, \beta, \gamma) | \Psi_i(\mathbf{Q}) \rangle.$$

In this expression we have used Born-Oppenheimer wave functions for the initial and final states, a dipole approximation to the matter-radiation interaction Hamiltonian, and the Condon approximation. Electronic wave functions are denoted by $\phi_f(\mathbf{x}, \mathbf{Q})$ and $\phi_i(\mathbf{x}, \mathbf{Q})$, where \mathbf{x} are the electronic coordinates in the body-fixed system, and \mathbf{Q} denotes the nuclear coordinates. The bar over the \mathbf{Q} in $\langle \phi_f(\mathbf{x}, \mathbf{Q}) | \sum_j x_{jM''} | \phi_i(\mathbf{x}, \mathbf{Q}) \rangle$ indicates that this electronic matrix element is to be evaluated at some averaged value of nuclear coordinates, perhaps specified by the \mathbf{Q} -centroid method.³⁷ Nuclear wave functions are specified by $\Psi_f(\mathbf{Q})$ and $\Psi_i(\mathbf{Q})$, and (α, β, γ) are the Euler angles of Sec. II which specify the orientation of the equilibrium axis in the bound electronic state.

The initial state wave function of Eq. (IV.1) is identical to that of Eq. (II.3), since we are interested in the angular distributions arising from well-defined states of this form. On the other hand, Eq. (II.7) cannot be used for Ψ_f , because we wish to consider transitions to states having only outgoing waves in the direction specified by $(\hat{\theta}, \hat{\phi})$.

The imposition of the correct boundary conditions on Ψ_f introduces an apparent paradox whose resolution is somewhat subtle. On the one hand, Ψ_f should be a pure outgoing wave, with no incoming flux, since this corresponds to the physical process of photofragmentation. On the other hand, matrix elements such as Eq. (IV.1) only make sense if Ψ_f is regular at the origin. No solution Ψ_f exists which is both a pure outgoing wave and is regular at the origin.

This problem has been carefully investigated by Band, Freed, and Kouri,⁴⁰ who have set up the photodissociation problem by explicitly considering the full Hamiltonian with coupling between the initial and final states. To lowest order in this coupling, they find that the dissociative wave function possesses only outgoing waves, but the amplitude of each outgoing wave is given by a matrix element involving the standing wave solution which is regular at the origin.

The appropriate wave function for use in evaluating

this amplitude Eq. (IV.1) is⁴⁰

$$\Psi_f^R(\mathbf{Q}) = \left\{ \sum_{i\mu} i^i e^{-i\delta_i} \psi_{E_i}(Q'_i) Y_{i\mu}(\theta_{SF}, \phi_{SF}) \right. \\ \left. \times Y_{i\mu}^*(\hat{\theta}, \hat{\phi}) \right\} Y_{jm}(\beta', \alpha') \psi_n(Q'_2), \quad (IV.2)$$

where we have assumed that the final molecular state possesses no electronic angular momentum. In Eq. (IV.2) $\psi_{E_i}(Q'_i)$ is the regular standing wave solution, with phase shift δ_i determined by the asymptotic requirement

$$\psi_{E_i}(Q'_i) \rightarrow \frac{1}{kQ'_i} \sin\left(kQ'_i - \frac{l\pi}{2} + \delta_i\right). \quad (IV.3)$$

Pursuing the asymptotic analysis for the two surface problem results in the asymptotic behavior of the upper surface wave function as⁴⁰

$$\Psi_f(\hat{\theta}, \hat{\phi}) \rightarrow \frac{e^{ikQ'_i}}{kQ'_i} Y_{jm}(\beta', \alpha') \psi_n(Q'_2) \langle \Psi_f^R(Q') | V | \Psi_i(\mathbf{Q}) \rangle, \quad (IV.4)$$

where $\Psi_f^R(Q')$ in the matrix element of Eq. (IV.4) is the regular solution Eqs. (IV.2) and (IV.3), while the physical wave function (IV.4) contains pure outgoing waves in the $(\hat{\theta}, \hat{\phi})$ direction. The photodissociation angular distribution is obtained as the modulus squared of the coefficient of $(Q'_i)^{-1} \exp(ikQ'_i) \psi_n(Q'_2) Y_{jm}(\beta', \alpha')$ and the detailed analysis is given in Appendix C.

Photodissociations involving nonzero electronic angular momentum are considerably more difficult to treat, and are not completely understood even in the case of diatomic molecule photodissociation. Hence, for the remainder of this section we consider only cases involving no electronic angular momentum both in the initial and final states. Under this limitation, electronic selection rules limit Eq. (IV.1) so that only contributions from $M''=0$ occur.

As described in Appendix A, the index q denotes the state of polarization of the incoming photon. For linearly polarized light $q=0$, and the z axis is taken to be the direction of photon polarization. The angles $(\hat{\theta}, \hat{\phi})$ are measured relative to the direction of polarization. Circularly polarized light propagating in the z direction corresponds to $q=\pm 1$, and the angles $(\hat{\theta}, \hat{\phi})$ are now measured relative to the axis of propagation of the light. Experiments are usually performed with light of well-defined polarization, so we drop the sum over q in Eq. (IV.1) and consider only the case of well-defined photon polarization. Thus, the probability of obtaining photofragments at position $(\hat{\theta}, \hat{\phi})$ in states specified by j , m , and n_2 is given by the golden rule

$$I_{fi}(\hat{\theta}, \hat{\phi}) = |e_q X_0|^2 |\langle \Psi_f(\mathbf{Q}) | D_{q0}^{1*}(\alpha, \beta, \gamma) | \Psi_i(\mathbf{Q}) \rangle|^2,$$

where

$$X_0 = \langle \phi_f(\mathbf{x}, \mathbf{Q}) | \sum_j x_{j0} | \phi_i(\mathbf{x}, \mathbf{Q}) \rangle. \quad (IV.5)$$

Considerable amounts of angular momentum algebra and rotation transformations^{42, 59} may be performed on Eq. (IV.5), as detailed in Appendix C, to obtain the relatively simple form

$$\begin{aligned}
I_{fi}(\hat{\theta}, \hat{\phi}) = & |e_q X_0|^2 \left(\frac{2j+1}{8\pi} \right) \sum_{\substack{l'l''m'' \\ J'J''n}} i^{l'-l} e^{i(\theta_1 - \theta_2)} (2l+1)(2l'+1)(2n+1)(2J'+1)(2J''+1) P_n(\cos\hat{\theta}) (-1)^{n+j+m''+q+J-J'+J''} \\
& \times W(l' l'' J'; nj) W(11 J' J''; nJ) \begin{pmatrix} l & l' & n \\ 0 & 0 & 0 \end{pmatrix} \begin{pmatrix} n & 1 & 1 \\ 0 & -q & q \end{pmatrix} \begin{pmatrix} l & j & J' \\ 0 & m'' & -m'' \end{pmatrix} \\
& \times \begin{pmatrix} l' & j & J'' \\ 0 & m' & -m' \end{pmatrix} \begin{pmatrix} J & 1 & J' \\ k & 0 & -k \end{pmatrix} \begin{pmatrix} J & 1 & J'' \\ k & 0 & -k \end{pmatrix} T_{J' j k m''} T_{J'' j k m'} , \tag{IV.6}
\end{aligned}$$

where the internal portion of the transition amplitude is

$$T_{J' j k m''} = \langle \psi_{E1}(Q'_1) \psi_n(Q'_2) d_{km''}^{J'}((\eta - \rho)\delta) | d_{m''0}^J(\eta\delta) \psi_{n_1}(Q_1) \psi_{n_2}(Q_2) \psi_n^k(\delta) \rangle . \tag{IV.7}$$

Here $W(l' l'' J'; nj)$ is a Racah coefficient,^{42,59} $\begin{pmatrix} l & l' & n \\ 0 & 0 & 0 \end{pmatrix}$, etc. are 3- j symbols,^{42,59} and $P_n(\cos\hat{\theta})$ is a Legendre polynomial.⁴³ Equation (IV.6) is derived from Eq. (IV.5) by summing over fragment diatomic molecule m sublevels and by averaging over the M sublevels of the initial state of the triatomic molecule. These quantum numbers are rarely determined in experiments, since magnetic fields are required to remove their degeneracy. Some information may be obtained by measuring the polarization of radiation emitted by the photofragments, and the present theory could be readily extended to calculate these polarization properties. However, we restrict ourselves to cases where magnetic sublevels are not resolved in order to greatly simplify the form of Eq. (IV.6).

Several general features of photofragment angular distributions are now apparent in Eq. (IV.6). First, the distributions show no dependence on the angle $\hat{\phi}$. This is of course to be expected, because the system under study is cylindrically symmetric. Consider a gas of randomly oriented molecules (all M sublevels equally probable) which is photodissociated into fragments by a photon with a well-defined axis of polarization or propagation. The orientation of the fragments is of no interest to us (the M sublevels are unresolved), so there is nothing in the problem to make one value of $\hat{\phi}$ different from any other, and of course there can be no $\hat{\phi}$ dependence in the result.

The 3- j symbol $\begin{pmatrix} n & 1 & 1 \\ 0 & -q & q \end{pmatrix}$ in Eq. (IV.6) serves to limit n

to the values 0, 1, or 2. This is a characteristic of the treatment of the interaction as a first-rank tensor, or dipole, coupling. In general,⁴⁶ interactions involving p -rank tensor couplings with randomly oriented initial states and products whose orientations are of no interest limit n to values of 0, 1, ..., $2p$. Thus, for example, a two-photon photodissociation or photoionization yields contributions to the angular distributions with values of n ranging from 0 to 4.

In order to simplify Eq. (IV.6) further, we consider the case of relatively high photofragment translational energy. Under these conditions $\psi_{E1}(Q'_1)$ varies only weakly with l , and this dependence is neglected. Furthermore, in the high-energy limit, the l dependence of the phase shifts δ_l , is of the form

$$\delta_l \sim \frac{l\pi}{2} - C , \tag{IV.8}$$

where C is a constant dependent on E , but not l . Most photodissociation experiments involve high enough energies to make these approximations valid, often with several thousand wave numbers of energy released into translation. The relatively infrequent case of a direct photodissociation just above threshold requires the use of the full Eq. (IV.6).

The relatively simple dependence of Eq. (IV.6) on l and l' permits the sums over l , l' , and m'' to be evaluated in this high-energy limit (see Appendix C), and integration over all values of $\hat{\phi}$ may be performed to obtain the high energy angular distribution

$$\begin{aligned}
I_{fi}(\hat{\theta}) = & |e_q X_0|^2 \left(\frac{2j+1}{4} \right) \sum_{\substack{J'J'' \\ m''n}} (2n+1)(2J'+1)(2J''+1) P_n(\cos\hat{\theta}) (-1)^{m''+J''+q+J-J'} W(11 J' J''; nJ) \\
& \times \begin{pmatrix} n & 1 & 1 \\ 0 & -q & q \end{pmatrix} \begin{pmatrix} J & 1 & J' \\ k & 0 & -k \end{pmatrix} \begin{pmatrix} J & 1 & J'' \\ k & 0 & -k \end{pmatrix} \begin{pmatrix} J'' & n & J' \\ -m' & 0 & m' \end{pmatrix} T_{J' j k m''} T_{J'' j k m'} . \tag{IV.9}
\end{aligned}$$

Since n is restricted to 0, 1, and 2, it is readily apparent that Eq. (IV.9) may be written in the form

$$I_{fi}(\hat{\theta}) = I_0 [1 + \alpha P_1(\cos\hat{\theta}) + \beta P_2(\cos\hat{\theta})] . \tag{IV.10}$$

It is the state-to-state values of α and β that we wish to examine now.

B. Results

Figures 13-15 display the calculated values of the coefficient β of Eq. (IV.10) for state-to-state photodissociation of HCN. The calculations are performed using

the high energy limit of Eq. (IV.9), assuming linearly polarized light ($q=0$) and a transition dipole parallel to the principal axis of inertia. The high energy limiting form (IV.9) corresponds to the "axial recoil" limit of Zare,³ since so much energy is released that the direc-

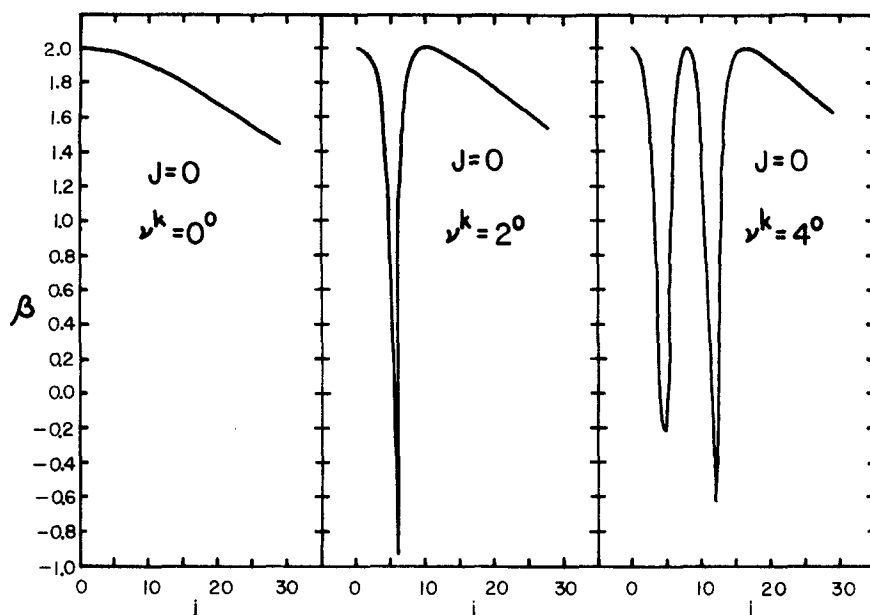


FIG. 13. State-to-state photofragment angular distribution coefficients β for HCN ($\rho=0.15268$, $\eta=0.63178$, $\kappa=4.1763$) in the high energy limit. These angular distributions are for HCN initially nonrotating ($J=0$), in bending vibrational states $\nu^k=0^0$, 2^0 , and 4^0 , producing CN fragments with rotational quantum number j .

tion of recoil of the departing fragments is along the axis connecting their centers of mass. Zare³ predicts that under these conditions, for a parallel transition and linearly polarized light, $\beta=2$.

A quick glance at Figs. 13–15 show that although β

approaches 2, there can be considerable deviation, especially for nonrotating initial states of the molecule. For example, for HCN initially in its $\nu^k=2^0$, $J=0$ state we calculate β for CN rotational state $j=6$ to be $-0.94!$

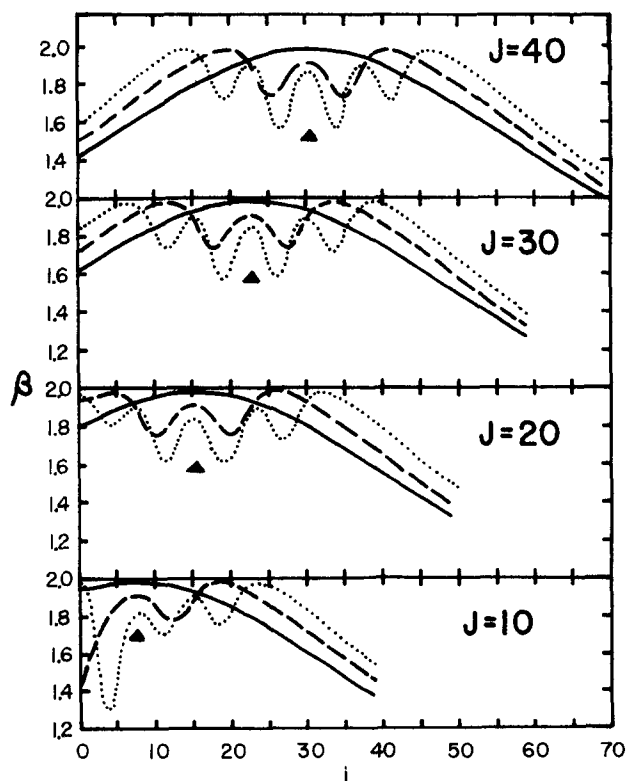


FIG. 14. State-to-state photofragment angular distribution coefficients β for HCN ($\rho=0.15268$, $\eta=0.63178$, $\kappa=4.1763$) in the high energy limit, for various states of total angular momentum J . Bending-vibrational states $\nu^k=0^0$, 2^0 , and 4^0 are indicated by solid, dashed, and dotted lines, respectively. The classical value of fragment rotational quantum number j^* is indicated by \blacktriangle .

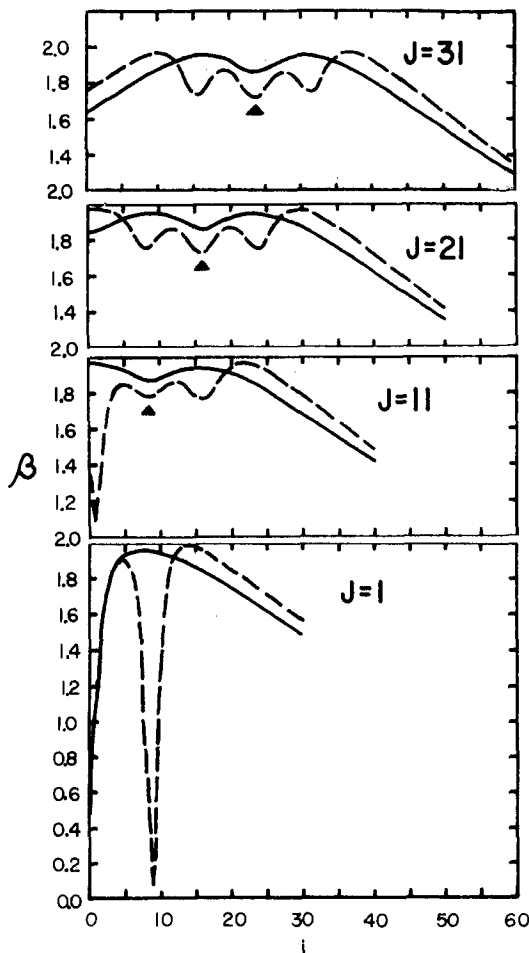


FIG. 15. Same as Fig. 14, but for HCN initially in its $\nu^k=1^1$ and 3^1 bending states. See note on Fig. 4.

This is a considerable departure from the axial recoil model.

Another feature of these state-to-state angular distributions which we observe is that as J becomes very large, the state-to-state angular distribution coefficients $\beta_j(j)$ become nearly symmetric about the classical value $j^* = [(\eta - \rho)/\eta]J$, which is indicated by triangles in the figures. Near this value of j , $\beta_j(j)$ is close to its classical, axial recoil value of 2, but undergoes oscillations as a function of j (for excited bending modes), then decays away from $\beta = 2$ as $|j - j^*|$ increases.

In Sec. III, we demonstrated that j^* is the preferred classical value for the photodissociation of a rigid (non-bending) triatomic molecule. As such, it corresponds to the case of axial recoil (as discussed by Zare³), so the $\beta(j^*) \approx 2$ results are readily understood. As j begins to depart from j^* , however, the angular momentum defect $|j - j^*|$ must be taken up in orbital motion. This requires an off-axis recoil, leading to increased isotropy of the angular distribution, and this is the cause of the decay of $\beta(j)$ from the value $\beta = 2$ at large $|j - j^*|$.

A comparison of these plots of $\beta_j(j)$ and the photofragment rotational distributions $P_j(j)$ for HCN (Figs. 3-7) shows that the extreme departures from axial recoil for $J = 0$ occur at nodes in the probability distribution $P_j(j)$, and thus are seldom to be observed. Furthermore, even the oscillations in $\beta_j(j)$ for J greater than zero correspond to oscillations in $P_j(j)$, with the largest departures of $\beta_j(j)$ from the axial recoil limit occurring with relatively lower probability.

We have also performed similar calculations for the photodissociation of ICN, but a graphical portrayal of the results is unnecessary. The calculated values of $\beta_j(j)$ for ICN are between 2.0 and 1.96 for all values of J and j except at isolated nodes in the distributions $P_j(j)$. The general shape of the curve $\beta_j(j)$ is found to be the same as that for HCN, except all the oscillations and large $|j - j^*|$ decays are much smaller.

It is evident, then, that deviations from the axial recoil limit are much larger for HCN than they are for ICN. We can understand this in terms of a semiclassical theory of photofragment angular distributions developed by Bersohn and co-workers.^{46,47,50,51} In this work Bersohn has shown that β is given by

$$\beta = 2 P_2(\cos\chi) \quad (\text{IV. 11})$$

for parallel transitions, where χ is the angle between the transition dipole moment and the axis giving the direction of departure of the fragments. For axial recoil, the fragments depart along the line connecting their centers of mass. If a molecule is constrained to be linear, this recoil direction would always be coincident with the molecular axis, and hence the transition dipole (for parallel transitions). As a linear triatomic molecule undergoes bending vibrations, however, the equilibrium principal axis of inertia (which we are considering to be identical with the transition dipole axis) deviates from the line connecting the fragment centers of mass. In fact, Fig. 2 shows that the angle χ between these two axes is given by

TABLE I. Comparison of averaged values of β by the weighted average of Eq. (IV. 9) to the value given by Eq. (IV. 15).

Molecule	Eq. (IV. 9)	Eq. (IV. 15)
HCN (0^0)	1.961	1.961
HCN (1^1)	1.923	1.921
HCN (2^0)	1.886	1.882
HCN (3^1)	1.849	1.842
HCN (4^0)	1.814	1.803
ICN (0^0)	1.99989	1.99988
ICN (1^1)	1.99977	1.99977
ICN (2^0)	1.99966	1.99965
ICN (3^1)	1.99954	1.99954
ICN (4^0)	1.99943	1.99942

$$\chi = \theta - \phi = (\eta - \rho)\delta \quad (\text{IV. 12})$$

Thus, if we consider the molecule to be undergoing bending vibrations, we expect the average value of β to be given by the expectation value of $2 P_2(\cos\chi)$. Small amplitude vibrations enable the use of the small angle limit in which this average yields

$$\bar{\beta} = 2 - 3(\eta - \rho)^2 \langle \delta^2 \rangle \quad (\text{IV. 13})$$

A calculation of $\langle \delta^2 \rangle$ is trivial for a harmonic oscillator. Application of the virial theorem yields

$$\langle \delta^2 \rangle = \frac{\nu + 1}{\kappa^2} \quad (\text{IV. 14})$$

so Eq. (IV. 13) becomes

$$\bar{\beta} = 2 - 3 \left(\frac{\eta - \rho}{\kappa} \right)^2 (\nu + 1) \quad (\text{IV. 15})$$

We have calculated average values of β , weighted by the probabilities $P_j(j)$, for various values of ν , k , and J for both HCN and ICN. The results are remarkably independent of J . Table I shows a comparison of the calculated averages and expression (IV. 15) for HCN and ICN in various initial bending states. The degree to which the two calculations agree is excellent, and indicates that Bersohn's formula is quite useful, even for the consideration of molecules which are undergoing bending vibrations provided the recoil direction is reinterpreted as arising from the molecule at its rms bent configuration.

Equation (IV. 15) also enables us to guess what molecules will be likely to exhibit large deviations from the axial recoil limit $\beta = 2$, simply from a knowledge of their masses, bond lengths, and bending vibrational frequency. Specifically, molecules with large amplitude bending motions (small κ) and light fragment atoms relative to the diatomic fragment (large $\eta - \rho$) dissociating from excited bending states (large ν) can be expected to give the largest departures from the purely axial recoil ($\beta = 2$) limit. With Eq. (IV. 15) in hand, and a knowledge of the parameters η , ρ , and κ for ICN, it is apparent that the angular distribution coefficients $\beta_j(j)$ for ICN are totally uninteresting. Of course, Eq. (IV. 15) is of no use in predicting the precise oscillations of the $\beta_j(j)$ curves.

Throughout this section, we have made one assumption, which should be spelled out quite clearly. We have

assumed that as the molecule bends, the transition dipole vector remains directed along the principal axis of the instantaneously bent molecule. In fact, as soon as the molecule is bent, the rigid selection rules defining parallel and perpendicular transitions break down, and transitions must be reclassified according to whether the transition dipole lies within the plane of the instantaneously bent molecule, or is perpendicular to it. There is nothing inherent in the theory as we have presented it which makes this assumption necessary. In fact, we could express the transition dipole in a coordinate system rotating with the principal axes of the triatomic molecule as an explicit function of δ (and possibly Q_1, Q_2), and then carry out all the required integrals. For small amplitude vibrations the resulting expression for the electronic matrix element could readily be expanded in a Taylor series about $\delta = 0$, and this series then would be rapidly convergent. The correction terms arising from nonzero powers of δ are generally expected to be small. We have simply chosen the model in which the transition dipole is always directed along the principal axis for purposes of definiteness.

As this juncture, a few more comments regarding Eqs. (IV.9) and (IV.10) are appropriate. Up to this point we have considered only photodissociations induced by linearly polarized light ($q=0$). Expression (IV.9) shows a dependence on the nature of the excitation, and it is readily shown that the coefficients β obtained for circularly polarized light ($q=\pm 1$) are related to those obtained for linearly polarized light by

$$\beta_{q=\pm 1} = -\frac{1}{2}\beta_{q=0}. \quad (\text{IV.16})$$

In addition, despite the form of Eqs. (IV.9) and (IV.10), we have as yet said nothing about the $\alpha P_1(\cos\theta)$ term in Eq. (IV.10). This is because, in practice, it is never observed. For $k=0$, consideration of the $3-j$ symbols $\begin{pmatrix} j & 1 & j' \\ k & 0 & -k \end{pmatrix}$ and $\begin{pmatrix} j'' & n & j' \\ m'' & 0 & m' \end{pmatrix}$ and the dependence of $T_{j'jk m'}$ on the sign of m' shows that $\alpha = 0$. For $k \neq 0$, α can take on nonzero values, but the value of α for a positive k is exactly the negative of that of α for negative k . Thus, for a sample with the degenerate states $k = \pm |k|$ equally populated, no net value of α can be detected. If L -type doubling is considered, the degeneracy of $k = \pm |k|$ levels is lifted, and linear combinations of the wave functions corresponding to definite signed values of k must be used, of the form

$$\psi = \frac{1}{\sqrt{2}}(|k\rangle \pm |-k\rangle), \quad (\text{IV.17})$$

to evaluate α . State selection of these even or odd parity states is difficult (although possible in principle in a double resonance experiment). In any case, it may be readily shown that in the absence of state selection, no nonzero value of α is obtained, even if the other quantum numbers J, ν, n_1, n_2, n , and j are state selected and state analyzed.

V. CONCLUSION

Using rigid rotor harmonic oscillator basis functions to describe the initially bound state of a linear triatomic molecule and rigid, free rotor-harmonic-oscillator basis functions with a wave function to describe unbound

states of the molecule, we have constructed a Franck-Condon theory of linear triatomic molecule photodissociations. These Franck-Condon factors enter prominently in the full theory of Band, Freed, and Kouri⁴⁰ which includes inelastic scattering on the unbound surface. The Franck-Condon factors have wave functions expressed in terms of the essentially different nuclear coordinates of the initial bound and the final dissociative potential energy surfaces. Nevertheless, these Franck-Condon integrals have been reduced to one-dimensional integrals, so the problem has been made analytically tractable.

We have investigated the case in which scattering events on the unbound surface are of negligible importance, and have shown that the small deviations of the diatomic axis from the equilibrium axis of the bound triatomic molecule can profoundly alter the calculated rotational, orbital angular momentum and angular distributions.

This effect, which we have termed dynamical axis switching, is unimportant for small values of total angular momentum J but becomes significant as J increases. It is also relatively less important for light atomic fragments, and becomes larger as the fragment atom increases in mass relative to the mass of the diatomic fragment. The parameter ρ of Eq. (II.19) ($0 \leq \rho \leq 1$) and the triatomic angular momentum J determine the magnitude of the dynamic axis switching phenomena through the combination $(J + \frac{1}{2})\rho$. As $(J + \frac{1}{2})\rho \rightarrow 0$ dynamic axis switching effects vanish, and these effects grow with $(J + \frac{1}{2})\rho$.

For high J , we have shown that the rotational-bending Franck-Condon factor alone predicts rotational and angular momentum distributions peaked about the classical values l^* and j^* , but exhibiting structure arising from the nodes in the bending wave function for the initially bound state of the molecule. The structure of these distributions is quite analogous to the results of the previous theory which ignored the dynamical axis switching, provided distributions arising from an initial total angular momentum J are compared to distributions arising from an effective total angular momentum J^* , which is determined by the dynamical axis switching phenomenon.

We have calculated state-to-state photofragment angular distribution coefficients β , and have demonstrated that in the high energy limit, the axial recoil approximation is usually valid. In particular, β for production of diatomic fragments in the classical rotational state specified by j^* is close to the axial recoil limit for parallel transitions of 2. As j deviates from j^* , increased isotropy in the state-to-state angular distributions arises because the angular momentum defect $|j - j^*|$ prohibits purely axial recoil.

Furthermore, we have shown that the state-averaged angular distributions deviate from the classical axial recoil value $\beta=2$. This result is a consequence of the fact that the vibrating linear molecule is bent on average,⁶⁰ and the angle χ between the transition dipole and dissociation direction has a nonzero root-mean squared aver-

age value. Thus, Bersohn's semiclassical formula $\beta = 2P_2(\cos\chi)$ has been verified for molecules undergoing bending vibrations, provided the expectation value of $P_2(\cos\chi)$ is used, rather than its equilibrium value.

ACKNOWLEDGMENT

The authors wish to thank Professor Yehuda Band of the Ben-Gurion University of the Negev, Beer-Sheva, Israel for helpful suggestions and his critical reading of this manuscript.

APPENDIX A: TENSOR AND ANGULAR MOMENTUM ALGEBRA FOR LINEAR TRIATOMIC MOLECULE PHOTODISSOCIATIONS

I. Direct photodissociation using a first-rank tensor coupling operator

Using Born-Oppenheimer wave functions for the initial and final states, the golden rule of time dependent perturbation theory, and a dipole approximation to the matter-radiation interaction Hamiltonian, the required matrix element $\langle f|V|i\rangle$ for direct photodissociation is

$$\langle f|V|i\rangle = \langle \Psi_f(\mathbf{Q}') | \hat{\mathbf{e}} \cdot \langle \phi_f(\mathbf{x}, \mathbf{Q}') | \sum_j \mathbf{r}_j | \phi_i(\mathbf{x}, \mathbf{Q}) \rangle_x | \Psi_i(\mathbf{Q}) \rangle, \quad (\text{A1})$$

where $\hat{\mathbf{e}}$ is the polarization of the photon, \mathbf{x} are the electronic coordinates in the body-fixed system, and \mathbf{r} are the electronic coordinates in the space-fixed system. By expressing $\hat{\mathbf{e}}$ and \mathbf{r}_j in spherical components with basis vectors $\hat{u}_{x1} = \mp(\hat{u}_x \pm i\hat{u}_y)/\sqrt{2}$, $\hat{u}_0 = \hat{u}_z$ ($\hat{u}_x, \hat{u}_y, \hat{u}_z$ denote unit vectors), we obtain

$$\langle f|V|i\rangle = \sum_{q=-1}^1 (-1)^q \hat{e}_q \langle \Psi_f(\mathbf{Q}') | \times \langle \phi_f(\mathbf{x}, \mathbf{Q}') | \sum_j r_{jq} | \phi_i(\mathbf{x}, \mathbf{Q}) \rangle_x | \Psi_i(\mathbf{Q}) \rangle. \quad (\text{A2})$$

Now, r_{jq} is a spherical tensor of the first rank. It transforms according to well-known rules under rotations Ref. 59, Eq. (4.5). Under the conventions of Brink and Satchler, a rotation by the Eulerian angles $(-\gamma, -\beta, -\alpha)$ takes the space-fixed coordinates into body-fixed coordinates, so

$$\begin{aligned} \Psi_f(\mathbf{Q}') &= \psi_n(Q'_2) \psi_{E1}(Q'_1) \left[\frac{(2l+1)(2j+1)}{(4\pi)^2} \right]^{1/2} \sum_{\mu m m' J'} \langle \hat{J} \hat{M} | l j \mu m \rangle \\ &\times \langle J' \mu + m | l j \mu m \rangle \langle J' m'' | l j m'' 0 \rangle D_{\mu+m, m}^{J' * *}(\alpha', \beta', \gamma') D_{0m}^l(0, \theta, 0). \end{aligned} \quad (\text{A11})$$

Use of Eqs. (A7)-(A9) and (A11) in Eq. (A6) thus produces

$$\begin{aligned} V_{fi}^{M''q} &= \sum_{\mu m m'} \langle \hat{J} \hat{M} | l j \mu m \rangle \langle J' \mu + m | l j \mu m \rangle \langle J' m'' | l j m'' 0 \rangle \left[\frac{(2l+1)(2j+1)(2J+1)}{8\pi^2(4\pi)^2} \right]^{1/2} \\ &\times \int d\Omega D_{\mu+m, m}^{J' * *}(\Omega) D_{q m m'}^{1 * *}(\Omega) D_{M'' m}^{J' * *}(\Omega) \langle \psi_n(Q'_2) \psi_{E1}(Q'_1) | d_{0m}^l(\theta) | d_{\mu+m}^l(\phi) | d_{km}^l(\phi) \psi_{n_1}(Q_1) \psi_{n_2}(Q_2) \psi_{\nu}^k(\delta) \rangle. \end{aligned} \quad (\text{A12})$$

Utilizing well-known expressions for integrals of products of D functions, and sum rules for Clebsch-Gordan coef-

$$\begin{aligned} \langle f|V|i\rangle &= \sum_{q=-1}^1 (-1)^q \hat{e}_q \sum_{M''} \langle \Psi_f(\mathbf{Q}') | D_{M''q}^{1 * *}(-\gamma, -\beta, -\alpha) \\ &\times \langle \phi_f(\mathbf{x}, \mathbf{Q}') | \sum_j x_{jM''} | \phi_i(\mathbf{x}, \mathbf{Q}) \rangle_x | \Psi_i(\mathbf{Q}) \rangle, \end{aligned} \quad (\text{A3})$$

where $D_{M''q}^{J * *}$ are the well-known rotation matrices. Invoking a Condon approximation yields

$$\begin{aligned} \langle f|V|i\rangle &= \sum_{q=-1}^1 (-1)^q \hat{e}_q \sum_{M''} \langle \Psi_f(\mathbf{Q}') | D_{M''q}^{1 * *}(-\gamma, -\beta, -\alpha) | \Psi_i(\mathbf{Q}) \rangle \\ &\times \langle \phi_f(\mathbf{x}, \mathbf{Q}') | \sum_j x_{jM''} | \phi_i(\mathbf{x}, \mathbf{Q}) \rangle_x. \end{aligned} \quad (\text{A4})$$

The subscript q indicates the polarization of the incoming photon. Circularly polarized light in the x - y plane has $q = \pm 1$, while $q = 0$ corresponds to light polarized in the z direction. Similarly, $M'' = 1$ for a perpendicular transition. We adopt the notation

$$X_{M''} = \langle \phi_f(\mathbf{x}, \mathbf{Q}') | \sum_j x_{jM''} | \phi_i(\mathbf{x}, \mathbf{Q}) \rangle_x, \quad (\text{A5})$$

$$V_{fi}^{M''q} = \langle \Psi_f(\mathbf{Q}') | D_{M''q}^{1 * *}(-\gamma, -\beta, -\alpha) | \Psi_i(\mathbf{Q}) \rangle. \quad (\text{A6})$$

In this derivation we consider only states of zero electronic angular momentum, thus avoiding problems of the coupling of Λ (or Ω) to k , and questions of the appropriate quantization of electronic angular momentum in the products. We use expressions (II.3) and (II.7) for Ψ_i and Ψ_f , respectively. Noting that

$$D_{M''q}^{1 * *}(-\gamma, -\beta, -\alpha) = D_{qM''}^{1 * *}(\alpha, \beta, \gamma) \quad (\text{A7})$$

[Ref. 42, Eq. (4.21)] and utilizing Eqs. (II.35) and (II.36) to convert (α, β, γ) and $(\phi_{SF}, \theta_{SF}, \gamma_{SF})$ to $(\alpha', \beta', \gamma')$ and δ , we obtain

$$\begin{aligned} \Psi_i(\mathbf{Q}) &= \left(\frac{2J+1}{8\pi^2} \right)^{1/2} \psi_{n_1}(Q_1) \psi_{n_2}(Q_2) \psi_{\nu}^k(\delta) \\ &\times \sum_{m'} D_{mM''}^{J * *}(\alpha', \beta', \gamma') D_{km}^J(0, \phi, 0), \end{aligned} \quad (\text{A8})$$

$$\begin{aligned} \Psi_f(\mathbf{Q}') &= \psi_n(Q'_2) \psi_{E1}(Q'_1) \left[\frac{(2l+1)(2j+1)}{(4\pi)^2} \right]^{1/2} \sum_{\mu m m'} \langle \hat{J} \hat{M} | l j \mu m \rangle \\ &\times D_{m0}^{J * *}(\alpha', \beta', \gamma') D_{\mu m m'}^{J * *}(\alpha', \beta', \gamma') D_{0m}^l(0, \theta, 0), \end{aligned} \quad (\text{A9})$$

$$D_{qM''}^{1 * *}(\alpha, \beta, \gamma) = \sum_{m''} D_{q m m''}^{1 * *}(\alpha', \beta', \gamma') D_{M'' m''}^1(0, \phi, 0). \quad (\text{A10})$$

The Clebsch-Gordan series for rotation functions⁴² may be substituted into Eq. (A9) to yield

ficients,⁴² we obtain

$$V_{fi}^{M''q} = \sum_{m''m'''} \langle \hat{J}m'' | ljm''0 \rangle \langle \hat{J}M + q | 1JqM \rangle \langle \hat{J}m'' | 1Jm''m'' \rangle \\ \times \left[\frac{(2l+1)(2j+1)(2J+1)}{2(2\hat{J}+1)^2} \right]^{1/2} \langle \psi_n(Q'_2) \psi_{E1}(Q'_1) d_{0m''}^l(\theta) | d_{km''}^j(\phi) | d_{km''}^j(\phi) \psi_{n_1}(Q_1) \psi_{n_2}(Q_2) \psi_v^k(\delta) \rangle. \quad (A13)$$

Further use of the Clebsch–Gordan series in (A13) and a Clebsch–Gordan sum rule⁴² then yields

$$V_{fi}^{M''q} = \left[\frac{(2l+1)(2j+1)(2J+1)}{2(2\hat{J}+1)^2} \right]^{1/2} \sum_{m''} \langle \hat{J}m'' | ljm''0 \rangle \\ \times \langle \hat{J}M + q | 1JqM \rangle \langle \hat{J}k + M'' | 1JM''k \rangle \langle \psi_n(Q'_2) \psi_{E1}(Q'_1) d_{0m''}^l(\theta) | d_{km''}^j(\phi) \psi_{n_1}(Q_1) \psi_{n_2}(Q_2) \psi_v^k(\delta) \rangle. \quad (A14)$$

In the case of zero electronic angular momentum in both electronic states, $M'' = 0$, and V_{fi} becomes

$$V_{fi}^{0q} = \left[\frac{(2l+1)(2j+1)(2J+1)}{2(2\hat{J}+1)^2} \right]^{1/2} \sum_{m''} \langle \hat{J}m'' | ljm''0 \rangle \\ \times \langle \hat{J}M + q | 1JqM \rangle \langle \hat{J}k | 1J0k \rangle \langle \psi_n(Q'_2) \psi_{E1}(Q'_1) d_{0m''}^l(\theta) | d_{km''}^j(\phi) \psi_{n_1}(Q_1) \psi_{n_2}(Q_2) \psi_v^k(\delta) \rangle. \quad (A15)$$

For photons of definite polarization, and ignoring the j dependence implicit in $\psi_{E1}(Q'_1)$ through energy conservation, it is possible to calculate the approximate photofragment orbital angular momentum distribution as

$$P_J(l) = \sum_j |e_q X_0|^2 |V_{fi}^{0q}|^2. \quad (A16)$$

Use of a Clebsch–Gordan sum rule then yields the result

$$P_J(l) = |e_q X_0|^2 \frac{(2l+1)(2J+1)}{2} \sum_{m''\hat{J}} \frac{1}{2\hat{J}+1} \\ \times [\langle \hat{J}k | 1J0k \rangle \langle \hat{J}M + q | 1JqM \rangle \langle \psi_n(Q'_2) \psi_{E1}(Q'_1) d_{0m''}^l(\theta) | d_{km''}^j(\phi) \psi_{n_1}(Q_1) \psi_{n_2}(Q_2) \psi_v^k(\delta) \rangle]^2. \quad (A17)$$

Determination of such a simple form for $P_J(j)$ seems hopeless at this point, but this is not the case. By solving Eqs. (II. 35) and (II. 36) for (α, β, γ) and $(\alpha', \beta', \gamma')$ in terms of $(\phi_{SF}, \theta_{SF}, \gamma_{SF})$ and δ , we obtain

$$D_{Mk}^j(\alpha, \beta, \gamma) = \sum_{m''} D_{m''}^j(\phi_{SF}, \theta_{SF}, \gamma_{SF}) D_{m''k}^j(0, \theta - \phi, 0), \quad (A18)$$

$$D_{mm}^j(\alpha', \beta', \gamma') = \sum_{m''} D_{m''}^j(\phi_{SF}, \theta_{SF}, \gamma_{SF}) D_{m''m}^j(0, \theta, 0). \quad (A19)$$

These transformations may be used on the wave functions (II. 3) and (II. 7), and on the coupling $D_{qm''}^{1*}(\alpha, \beta, \gamma)$ to provide expressions referred to a body-fixed system fixed relative to the diatom–atom vector. Manipulations entirely analogous to those given above then permit the calculation of $P_J(j)$, again ignoring the dependence of $\psi_{E1}(Q'_1)$ on l , yielding

$$P_J(j) = |e_q X_0|^2 \frac{(2j+1)(2J+1)}{2} \sum_{m''\hat{J}} \frac{1}{2\hat{J}+1} \\ \times [\langle \hat{J}k | 1J0k \rangle \langle \hat{J}M + q | 1JqM \rangle \langle \psi_n(Q'_2) \psi_{E1}(Q'_1) d_{0m''}^l(\theta) | d_{km''}^j(\theta - \phi) \psi_{n_1}(Q_1) \psi_{n_2}(Q_2) \psi_v^k(\delta) \rangle]^2. \quad (A20)$$

Of course, averaging over initial M levels may be analytically done, yielding for Eqs. (A17) and (A20)

$$P_J(l) = \frac{|e_q X_0|^2}{3} \left[\left(l + \frac{1}{2} \right) \sum_{m''\hat{J}} \langle \hat{J}k | 1J0k \rangle^2 \langle \psi_n(Q'_2) \psi_{E1}(Q'_1) d_{0m''}^l(\theta) | d_{km''}^j(\phi) \psi_{n_1}(Q_1) \psi_{n_2}(Q_2) \psi_v^k(\delta) \rangle \right]^2 \quad (A21)$$

and

$$P_J(j) = \frac{|e_q X_0|^2}{3} \left[\left(j + \frac{1}{2} \right) \sum_{m''\hat{J}} \langle \hat{J}k | 1J0k \rangle^2 \langle \psi_n(Q'_2) \psi_{E1}(Q'_1) d_{0m''}^l(\theta) | d_{km''}^j(\theta - \phi) \psi_{n_1}(Q_1) \psi_{n_2}(Q_2) \psi_v^k(\delta) \rangle \right]^2. \quad (A22)$$

II. Photodissociation by scalar coupling

Having obtained expressions for $\langle f | V | i \rangle$ with V a first-rank tensor, the case when it is a scalar is trivial. Formulas (A8) and (A9) may still be used, giving after some manipulation as above

$$\langle f | V | i \rangle = \left[\frac{(2l+1)(2j+1)}{2(2J+1)} \right]^{1/2} \bar{V} \delta_{j\hat{J}} \delta_{m\hat{M}} \sum_{m''} \langle \hat{J}m'' | ljm''0 \rangle \langle \psi_n(Q'_2) \psi_{E1}(Q'_1) d_{0m''}^l(\theta) | \psi_{n_1}(Q_1) \psi_{n_2}(Q_2) \psi_v^k(\delta) d_{km''}^j(\phi) \rangle \quad (A23)$$

as given in Eq. (II. 37a). Squaring and summing over j (ignoring the dependence of ψ_{E1} on j), we obtain the distribution of orbital angular momentum $P_J(l)$ as

$$P_J(l) = \bar{V}^2(l + \frac{1}{2}) \delta_{J\hat{J}} \delta_{M\hat{M}} \sum_{m'} |\langle \psi_n(Q_2') \psi_{E1}(Q_1') d_{0m}^l(\theta) | \psi_{n_1}(Q_1) \psi_{n_2}(Q_2) \psi_\nu^k(\delta) d_{km}^J(\phi) \rangle|^2. \quad (\text{A24})$$

As in the first section of this Appendix, we may also do the calculation referring everything to a body-fixed system rotating with the diatom-atom vector, to give

$$\langle f | V | i \rangle = \left[\frac{(2l+1)(2j+1)}{2(2J+1)} \right]^{1/2} \bar{V} \delta_{J\hat{J}} \delta_{M\hat{M}} \sum_{m''} \langle Jm'' | l j 0 m'' \rangle \langle \psi_n(Q_2') \psi_{E1}(Q_1') d_{m''}^l(\theta) | \psi_{n_1}(Q_1) \psi_{n_2}(Q_2) \psi_\nu^k(\delta) d_{m''}^J(\theta - \phi) \rangle \quad (\text{A25})$$

as given in Eq. (II. 37b). Then the distribution $P_J(j)$ may be obtained as

$$P_J(j) = \bar{V}^2(j + \frac{1}{2}) \delta_{J\hat{J}} \delta_{M\hat{M}} \sum_{m''} |\langle \psi_n(Q_2') \psi_{E1}(Q_1') d_{0m''}^j(\theta) | \psi_{n_1}(Q_1) \psi_{n_2}(Q_2) \psi_\nu^k(\delta) d_{m''}^J(\theta - \phi) \rangle|^2. \quad (\text{A26})$$

The similarity of Eqs. (A24) and (A21) and of Eqs. (A26) and (A22) shows that unless Eqs. (A22) and (A24) show a very strong dependence on J , the results including the first-rank tensorial coupling of Eqs. (A21) and (A22) differ only slightly from the scalar coupling calculation. This arises because the first-rank tensorial coupling distributions from an initial state specified by J_{tensor} are merely linear combinations of scalar coupling results for $J_{\text{scalar}} = J_{\text{tensor}}, J_{\text{tensor}} \pm 1$. Thus, the full dipole interaction need not be retained if rotational distributions are all that is desired. It is necessary, however, for a treatment of photofragment angular distributions.

APPENDIX B: EVALUATION OF LINEAR TRIATOMIC MOLECULE BENDING-ROTATION FRANCK-CONDON FACTORS

I. Amplitudes for joint production of j and l

Expression of Eq. (II. 40) for the bending-rotation Franck-Condon factor requires the evaluation of the sum of integrals

$$Z_{\nu k} = \eta \sum_{k'} \langle Jk' | l j k' 0 \rangle \int_0^\infty d\delta \delta d_{0k'}^l(\eta\delta) d_{kk'}^J(\rho\delta) \psi_\nu^k(\delta). \quad (\text{B1})$$

Using the Bessel approximations (II. 41) and (II. 42) and the symmetry $\langle Jk' | l j k' 0 \rangle = (-1)^{l+j-J} \langle J - k' | l j - k' 0 \rangle$, this may be rewritten as

$$Z_{\nu k} = \eta \kappa \sum_{k'=0} \langle Jk' | l j k' 0 \rangle (l + \frac{1}{2})^{-k'} (J + \frac{1}{2})^{-k} \left[\frac{(l+k')!(J+k_>)! 2 \left(\frac{\nu-k}{2}\right)!}{(l-k')!(J-k_>)! \left(\frac{\nu+k}{2}\right)!} \right]^{1/2} \left\{ (J + \frac{1}{2})^{k_<} \left[\frac{(J-k_<)!}{(J+k_<)!} \right]^{1/2} \right. \\ \times \int_0^\infty d\delta \delta (\kappa\delta)^k J_{k_<}((l + \frac{1}{2})\eta\delta) J_{|k-k_>}((J + \frac{1}{2})\rho\delta) L_{(\nu-k)/2}^k(\kappa^2\delta^2) \exp(-\kappa^2\delta^2/2) (-1)^{k-k_<} \\ \left. + (J + \frac{1}{2})^{-k_<} \left[\frac{(J+k_<)!}{(J-k_<)!} \right]^{1/2} (-1)^{l+j-J+k} \int_0^\infty d\delta \delta (\kappa\delta)^k J_{k_>}((l + \frac{1}{2})\eta\delta) J_{k_>}((J + \frac{1}{2})\rho\delta) L_{(\nu-k)/2}^k(\kappa^2\delta^2) \exp(-\kappa^2\delta^2/2) \right\}, \quad (\text{B2})$$

where the second term in the braces is omitted when $k'=0$, and $k_<$ and $k_>$ are taken to be the lesser and the greater of k and k' , respectively. The integrals remaining in Eq. (B2) are now quite involved, but the general results may be simplified using the identities

$$L_n^k(\kappa^2\delta^2) = \sum_{m=0}^n (-1)^m \binom{n+k}{n-m} \frac{(\kappa^2\delta^2)^m}{m!} \quad [\text{Ref. 43, (8.970.1)}], \quad (\text{B3})$$

$$(\kappa^2\delta^2)^m e^{-\kappa^2\delta^2/2} = \left(-\frac{\kappa}{2} \frac{d}{d\kappa} \right)^m e^{-\kappa^2\delta^2/2}, \quad (\text{B4})$$

$$\delta J_k(A\delta) = \left(\frac{d}{dA} + \frac{k+1}{A} \right) J_{k+1}(A\delta) \quad [\text{Ref. 43, (8.472.1)}], \quad (\text{B5})$$

$$\delta^n J_k(A\delta) = \left\{ \left(\frac{d}{dA} + \frac{k+1}{A} \right) \left(\frac{d}{dA} + \frac{k+2}{A} \right) \dots \left(\frac{d}{dA} + \frac{k+n}{A} \right) \right\} J_{k+n}(A\delta), \quad (\text{B6})$$

and the standard integral [Ref. 43, (6.633.2)]

$$\int_0^\infty d\delta \delta J_k(A\delta) J_k(B\delta) \exp(-\kappa^2\delta^2/2) = \frac{1}{\kappa^2} \exp\left(-\frac{A^2+B^2}{2\kappa^2}\right) I_k\left(\frac{AB}{\kappa^2}\right). \quad (\text{B7})$$

The integrals involved in Eq. (B2) are all of the form

$$W_{n k k' \Delta} = \int_0^\infty d\delta \delta (\kappa\delta)^k J_{k'}(A\delta) J_{k-\Delta}(B\delta) L_n^k(\kappa^2\delta^2) e^{-\kappa^2\delta^2/2}, \quad (\text{B8})$$

where $\Delta = k, k-2, k-4, \dots, 0$.

Application of formulas (B3)–(B7) then yields the following general solution for $W_{nkk'\Delta}$:

$$W_{nkk'\Delta} = \sum_{m=0}^n \binom{n+k}{n-m} \frac{(-1)^{(k-\Delta)/2} \kappa^k}{2^m m!} \left(\kappa \frac{d}{d\kappa} \right)^m \left(\frac{1}{\kappa} \frac{d}{d\kappa} \right)^{(k-\Delta)/2} \times \left\{ \left(\frac{d}{dB} + \frac{k' - \Delta + 1}{B} \right) \left(\frac{d}{dB} + \frac{k' - \Delta + 2}{B} \right) \cdots \left(\frac{d}{dB} + \frac{k'}{B} \right) \right\} \left[\frac{1}{\kappa^2} \exp \left(-\frac{A^2 + B^2}{2\kappa^2} \right) I_{k'} \left(\frac{AB}{\kappa^2} \right) \right]. \quad (\text{B9})$$

Using this result (B9), analytic forms for $Z_{\nu k}$ have been derived for $\nu^k = 0^0, 1^1, 2^0, 3^1,$ and 4^0 and are found to be

$$Z_{0^0} = \sqrt{2} \frac{\eta}{\kappa} [1 + (-1)^{l+j-J}] \exp \left(-\frac{A^2 + B^2}{2\kappa^2} \right) \sum_{p \geq 0} \langle Jp | lj p 0 \rangle [(l + \frac{1}{2})(J + \frac{1}{2})]^{-p} \frac{1}{1 + \delta_{p0}} \left[\frac{(l+p)!(J+p)!}{(l-p)!(J-p)!} \right]^{1/2} I_p(y), \quad (\text{B10})$$

$$Z_{2^0} = \sqrt{2} \frac{\eta}{\kappa} [1 + (-1)^{l+j-J}] \exp \left(-\frac{A^2 + B^2}{2\kappa^2} \right) \times \sum_{p \geq 0} \langle Jp | lj p 0 \rangle [(l + \frac{1}{2})(J + \frac{1}{2})]^{-p} \left[\frac{(l+p)!(J+p)!}{(l-p)!(J-p)!} \right]^{1/2} \left[(2x-1)I_p(y) - y(I_{p+1}(y) + I_{p-1}(y)) \right] \frac{1}{1 + \delta_{p0}}, \quad (\text{B11})$$

$$Z_{4^0} = \sqrt{2} \frac{\eta}{\kappa} [1 + (-1)^{l+j-J}] \exp \left(-\frac{A^2 + B^2}{2\kappa^2} \right) \sum_{p \geq 0} \langle Jp | lj p 0 \rangle [(l + \frac{1}{2})(J + \frac{1}{2})]^{-p} \left[\frac{(l+p)!(J+p)!}{(l-p)!(J-p)!} \right]^{1/2} \times \frac{1}{1 + \delta_{p0}} \left\{ (2x^2 - 4x + 1 + y^2)I_p(y) + y(2-2x)[I_{p+1}(y) + I_{p-1}(y)] + \frac{y^2}{2}[I_{p+2}(y) + I_{p-2}(y)] \right\}, \quad (\text{B12})$$

$$Z_{1^1} = \sqrt{2} \frac{\eta}{\kappa} \exp \left(-\frac{A^2 + B^2}{2\kappa^2} \right) \sum_{p \geq 1} \langle Jp | lj p 0 \rangle [(l + \frac{1}{2})(J + \frac{1}{2})]^{-p} \left[\frac{(l+p)!(J+p)!}{(l-p)!(J-p)!} \right]^{1/2} \frac{J + \frac{1}{2}}{\sqrt{J(J+1)}} \times \left\{ \frac{A}{2\kappa} [I_{p-1}(y) + I_{p+1}(y)] + \left(\frac{\rho\kappa}{B} - \frac{B}{\kappa} \right) I_p(y) \right\} + (-1)^{l+j-J+1} \langle Jp-1 | lj p-1 0 \rangle [(l + \frac{1}{2})(J + \frac{1}{2})]^{1-p} \times \left[\frac{(l+p-1)!(J+p-1)!}{(l-p+1)!(J-p+1)!} \right]^{1/2} \frac{\sqrt{J(J+1)}}{J + \frac{1}{2}} \left\{ \frac{B}{2\kappa} [I_{p-1}(y) + I_{p+1}(y)] + \left(\frac{p\kappa}{A} - \frac{A}{\kappa} \right) I_p(y) \right\}, \quad (\text{B13})$$

$$Z_{3^1} = \sqrt{2} \frac{\eta}{\kappa} \exp \left(-\frac{A^2 + B^2}{2\kappa^2} \right) \sum_{p \geq 1} \langle Jp | lj p 0 \rangle [(l + \frac{1}{2})(J + \frac{1}{2})]^{-p} \left[\frac{(l+p)!(J+p)!}{(l-p)!(J-p)!} \right]^{1/2} \frac{J + \frac{1}{2}}{\sqrt{J(J+1)}} \left\{ I_p(y) \left[\frac{p\kappa}{\sqrt{2}B} + \frac{\sqrt{2}B}{\kappa} (1-x) - \frac{Ay}{\sqrt{2}\kappa} \right] + [I_{p+1}(y) + I_{p-1}(y)] \frac{A}{\sqrt{2}\kappa} \left(x - p - 1 + \frac{B^2}{\kappa^2} \right) - \frac{Ay}{2\sqrt{2}\kappa} [I_{p+2}(y) + I_{p-2}(y)] \right\} + (-1)^{l+j-J+1} \langle Jp-1 | lj p-1 0 \rangle [(l + \frac{1}{2})(J + \frac{1}{2})]^{1-p} \times \left[\frac{(l+p-1)!(J+p-1)!}{(l-p+1)!(J-p+1)!} \right]^{1/2} \frac{\sqrt{J(J+1)}}{J + \frac{1}{2}} \left\{ I_p(y) \left[\frac{p\kappa}{\sqrt{2}A} + \frac{\sqrt{2}A}{\kappa} (1-x) - \frac{By}{\sqrt{2}\kappa} \right] + [I_{p+1}(y) + I_{p-1}(y)] \frac{B}{\sqrt{2}\kappa} \left(x - p - 1 + \frac{A^2}{\kappa^2} \right) - \frac{By}{2\sqrt{2}\kappa} [I_{p+2}(y) + I_{p-2}(y)] \right\}. \quad (\text{B14})$$

In these formulas I_p is the modified Bessel function,⁴³ and

$$A = \eta(l + \frac{1}{2}), \quad (\text{B15})$$

$$B = \rho(j + \frac{1}{2}), \quad (\text{B16})$$

$$x = (A^2 + B^2)/2\kappa^2, \quad (\text{B17})$$

$$y = AB/\kappa^2. \quad (\text{B18})$$

Expressions for other values of ν and k may be obtained from Eq. (B9) as desired. All of these expressions reduce to the correct limiting case (neglect of dynamic axis switching) as $\rho \rightarrow 0$.

II. Probabilities of producing $j(l)$ independent of $l(j)$

If one is only interested in the probability distributions for production of j (or l) independent of l (or j), formulas (III. 1) and (III. 2) are much simpler to deal with than Eq. (II. 40). Making the small angle Bessel approximation in Eq. (III. 1) then yields a sum of the squares of integrals of the form of Eq. (B8), and the general solution of these integrals (B9) then permits rapid computation. We have worked out these results explicitly for the cases $\nu^k = 0^0, 1^1, 2^0, 3^1,$ and 4^0 , thereby obtaining

$$P_J^{0^0}(l) = 2(2l+1) \left(\frac{\eta}{\kappa} \right)^2 \exp \left(-\frac{A^2 + B^2}{\kappa^2} \right) \left\{ \sum_{m=0}^{\min(J,l)} [(J + \frac{1}{2})(l + \frac{1}{2})]^{-2m} \left[\frac{(J+m)!(l+m)!}{(J-m)!(l-m)!} \right] [I_m(y)]^2 \frac{1}{1 + \delta_{m0}} \right\}, \quad (\text{B19})$$

$$P_J^{2^0}(l) = 2(2l+1) \left(\frac{\eta}{\kappa} \right)^2 \exp \left(-\frac{A^2 + B^2}{\kappa^2} \right) \left[\sum_{m=0}^{\min(J,l)} [(J + \frac{1}{2})(l + \frac{1}{2})]^{-2m} \times \left[\frac{(J+m)!(l+m)!}{(J-m)!(l-m)!} \right] \frac{1}{1 + \delta_{m0}} [I_m(y)(2x-1) - y(I_{m+1}(y) + I_{m-1}(y))]^2 \right], \quad (\text{B20})$$

$$P_J^4(l) = 2(2l+1) \left(\frac{\eta}{\kappa}\right)^2 \exp\left(-\frac{A^2+B^2}{\kappa^2}\right) \left(\sum_{m=0}^{\min(J,l)} [(J+\frac{1}{2})(l+\frac{1}{2})]^{-2m} \frac{[(J+m)!(l+m)!]}{[(J-m)!(l-m)!]}\right) \\ \times \frac{1}{1+\delta_{m0}} \left\{ (2x^2 - 4x + 1 + y^2) I_m(y) + y(2-2x)[I_{m+1}(y) + I_{l-m-1}(y)] + \frac{y^2}{2} [I_{m+2}(y) + I_{l-m-2}(y)] \right\}^2, \quad (\text{B21})$$

$$P_J^4(l) = (2l+1) \eta^2 \frac{J(J+1)}{(J+\frac{1}{2})^2} \exp\left(-\frac{A^2+B^2}{\kappa^2}\right) \left\{ \left[I_1(y) \left(\frac{1}{A} - \frac{A}{\kappa^2} \right) + [I_2(y) + I_0(y)] \frac{B}{2\kappa^2} \right]^2 + \sum_{m=1}^{\min(J,l)} (l+\frac{1}{2})^{-2m} \frac{[(l+m)!]}{[(l-m)!]} \right. \\ \times \left. \left((J+\frac{1}{2})^{2m} \frac{(J-m)!}{(J+m)!} \left[I_m(y) \left(\frac{m}{B} - \frac{B}{\kappa^2} \right) + [I_{m+1}(y) + I_{m-1}(y)] \frac{A}{2\kappa^2} \right]^2 \right. \right. \\ \left. \left. + (J+\frac{1}{2})^{-2m} \frac{(J+m)!}{(J-m)!} \left[I_{m+1}(y) \left(\frac{m+1}{A} - \frac{A}{\kappa^2} \right) + [I_{m+2}(y) + I_m(y)] \frac{B}{2\kappa^2} \right]^2 \right) \right\}, \quad (\text{B22})$$

$$P_J^4(l) = (l+\frac{1}{2}) \eta^2 \frac{J(J+1)}{(J+\frac{1}{2})^2} \exp\left(-\frac{A^2+B^2}{\kappa^2}\right) \left\{ \left[I_1(y) \left(\frac{2x}{A} - \frac{2xA}{\kappa^2} + \frac{2A-By}{\kappa^2} \right) + [I_2(y) + I_0(y)] \frac{B}{\kappa^2} \left(x - 2 + \frac{A^2}{\kappa^2} \right) \right. \right. \\ \left. \left. - \frac{By}{2\kappa^2} [I_3(y) + I_1(y)] \right\}^2 + \sum_{m=1}^{\min(J,l)} (l+\frac{1}{2})^{-2m} \frac{(l+m)!}{(l-m)!} \left((J+\frac{1}{2})^{2m} \frac{(J-m)!}{(J+m)!} \left[I_m(y) \left(\frac{2mx}{B} - \frac{2Bx}{\kappa^2} + \frac{2B-Ay}{\kappa^2} \right) \right. \right. \\ \left. \left. + [I_{m+1}(y) + I_{m-1}(y)] \frac{A}{\kappa^2} \left(x - 1 - m + \frac{B^2}{\kappa^2} \right) - \frac{Ay}{2\kappa^2} [I_{m+2}(y) + I_{l-m-2}(y)] \right]^2 + (J+\frac{1}{2})^{-2m} \frac{(J+m)!}{(J-m)!} \left[I_{m+1}(y) \left[\frac{2x(m+1)}{A} \right. \right. \right. \\ \left. \left. \left. - \frac{2xA}{\kappa^2} + \frac{2A-By}{\kappa^2} \right] + [I_{m+2}(y) + I_m(y)] \frac{B}{\kappa^2} \left(x - 2 - m + \frac{A^2}{\kappa^2} \right) - \frac{By}{2\kappa^2} [I_{m+3}(y) + I_{m-1}(y)] \right]^2 \right) \right\}. \quad (\text{B23})$$

Explicit expressions for other values of ν and k are readily obtained from Eq. (B9).

APPENDIX C: LINEAR TRIATOMIC MOLECULE PHOTOFRAGMENT ANGULAR DISTRIBUTIONS

Starting with Eq. (IV.5) and expressions (II.3) and (IV.2) for the wave functions Ψ_i and Ψ_f , we may convert the spherical harmonics to rotation matrices,⁴² use relations (A18) and (A19) to express (α, β, γ) and $(\alpha', \beta', \gamma')$ in terms of $(\phi_{\text{SF}}, \theta_{\text{SF}}, \gamma_{\text{SF}})$, and thereby obtain

$$I_{fi}(\hat{\theta}, \hat{\phi}) = |e_q X_0|^2 \frac{(2J+1)(2j+1)}{32\pi^3} \left| \sum_{\substack{i, \mu, m, m'' \\ m''=m}} i^{-i} e^{i\delta_i} \frac{(2l+1)}{4\pi} D_{\mu 0}^{i*}(\hat{\phi}, \hat{\theta}, 0) \int d\Omega_{\text{SF}} D_{\mu 0}^i(\Omega_{\text{SF}}) D_{m m''}^j(\Omega_{\text{SF}}) \right. \\ \left. \times D_{m m''}^{j*}(\Omega_{\text{SF}}) D_{m m''}^{1*}(\Omega_{\text{SF}}) \langle \psi_{E1}(Q'_1) d_{m'' 0}^{j*}(\theta) \psi_n(Q'_2) | d_{m'' 0}^{1*}(\theta - \phi) | d_{m'' 0}^{j*}(\theta - \phi) \psi_{n_1}(Q_1) \psi_{n_2}(Q_2) \psi_{\nu}^k(\delta) \rangle \right|^2. \quad (\text{C1})$$

Application of the Clebsch-Gordan series for D functions⁴² and an expression for the integral of a product of three D functions⁴² then yields

$$I_{fi}(\hat{\theta}, \hat{\phi}) = |e_q X_0|^2 \frac{(2J+1)(2j+1)}{8\pi} \left| \sum_{\substack{\mu, m, m'' \\ i, j, j''}} \langle J' \mu + m | l j \mu m \rangle \langle J' m'' | l j 0 m'' \rangle \right. \\ \left. \times \langle J' \mu + m | J 1 M q \rangle \langle J' m'' | J 1 m' m'' \rangle \langle J'' m' + m'' | J 1 m' m'' \rangle \langle J'' k | J 1 k 0 \rangle \right. \\ \left. \times i^{-i} e^{i\delta_i} \frac{2l+1}{2J'+1} D_{\mu 0}^{i*}(\hat{\phi}, \hat{\theta}, 0) \langle \psi_{E1}(Q'_1) \psi_n(Q'_2) d_{m'' 0}^{j*}(\theta) | d_{m'' 0}^{j''*}(\theta - \phi) \psi_{n_1}(Q_1) \psi_{n_2}(Q_2) \psi_{\nu}^k(\delta) \rangle \right|^2. \quad (\text{C2})$$

The Clebsch-Gordan coefficient $\langle J' m'' | J 1 m' m'' \rangle$ constrains $m' + m'' = m''$, so the sum over m' and m'' is simplified by the sum rule

$$\sum_{m', m''} \langle J' m'' | J 1 m' m'' \rangle \langle J'' m' + m'' | J 1 m' m'' \rangle = \delta_{J' J''}, \quad (\text{C3})$$

yielding

$$I_{fi}(\hat{\theta}, \hat{\phi}) = |e_q X_0|^2 \frac{(2J+1)(2j+1)}{8\pi} \left| \sum_{i, \mu, m, j'} i^{-i} e^{i\delta_i} \frac{2l+1}{2J'+1} \right. \\ \left. \times D_{\mu 0}^{i*}(\hat{\phi}, \hat{\theta}, 0) \langle J' \mu + m | l j \mu m \rangle \langle J' m'' | l j 0 m'' \rangle \langle J' \mu + m | J 1 M q \rangle \langle J' k | J 1 k 0 \rangle T_{J' j k m''} \right|^2, \quad (\text{C4})$$

where

$$T_{J' j k m''} = \langle \psi_{E1}(Q'_1) \psi_n(Q'_2) d_{m'' 0}^{j*}(\theta) | d_{k m''}^{j'}(\phi - \theta) \psi_{n_1}(Q_1) \psi_{n_2}(Q_2) \psi_{\nu}^k(\delta) \rangle, \quad (\text{C5})$$

as in Eq. (IV.7).

Noting that $\mu + m = M + q$, we see that only one value of μ may contribute to the sum. Explicitly squaring the sum in Eq. (C4) and utilizing the fact that⁵⁹

$$D_{\mu 0}^{l*}(\hat{\phi}, \hat{\theta}, 0) D_{\mu 0}^{l'}(\hat{\phi}, \hat{\theta}, 0) = (-1)^\mu \sum_n (2n+1) P_n(\cos \hat{\theta}) \begin{pmatrix} l & l' & n \\ \mu & -\mu & 0 \end{pmatrix} \begin{pmatrix} l & l' & n \\ 0 & 0 & 0 \end{pmatrix}, \quad (\text{C6})$$

we then obtain

$$I_{fl}(\hat{\theta}, \hat{\phi}) = |e_q X_0|^2 \frac{(2J+1)(2j+1)}{8\pi} \sum_{\substack{l'l''\mu n \\ m'm''J'J''}} i^{(l+l'')} e^{i(\delta_l - \delta_{l'})} (-1)^\mu P_n(\cos \hat{\theta}) \frac{(2n+1)(2l+1)(2l'+1)}{(2J'+1)(2J''+1)} \begin{pmatrix} l & l' & n \\ \mu & -\mu & 0 \end{pmatrix} \begin{pmatrix} l & l' & n \\ 0 & 0 & 0 \end{pmatrix} \\ \times T_{J'jkm''} T_{J''jkm'} \langle J' \mu + m | l j \mu m \rangle \langle J'' \mu + m | l' j \mu m \rangle \langle J' m'' | l j 0 m'' \rangle \\ \times \langle J'' m' | l' j 0 m' \rangle \langle J' \mu + m | J 1 M q \rangle \langle J'' \mu + m | J 1 M q \rangle \langle J' k | J 1 k 0 \rangle \langle J'' k | J 1 k 0 \rangle. \quad (\text{C7})$$

Equation (IV.6) may then be obtained by the conversion of all Clebsch-Gordan coefficients to 3-j symbols,⁵⁹ summation over final m sublevels and averaging over initial M -sublevels using the relation⁵⁹

$$W(abcd; ef) \begin{pmatrix} c & a & f \\ \gamma & \alpha & \phi \end{pmatrix} = \sum_{\beta\delta\epsilon} (-1)^{f-e-\alpha-\delta} \begin{pmatrix} a & b & e \\ \alpha & \beta & -\epsilon \end{pmatrix} \begin{pmatrix} d & c & e \\ \delta & \gamma & \epsilon \end{pmatrix} \begin{pmatrix} b & d & f \\ \beta & \delta & -\phi \end{pmatrix}. \quad (\text{C8})$$

Introduction of the high energy approximation to the phase shifts

$$\delta_l = \frac{l\pi}{2} - c \quad (\text{C9})$$

and taking $T_{J'jkm''}$ to be independent of l now permits further simplification of Eq. (IV.6), through the evaluation of the sums over l and l' . These summations may readily be performed using the relation⁵⁹

$$\begin{pmatrix} a & b & e \\ \alpha & \beta & -\epsilon \end{pmatrix} \begin{pmatrix} d & c & e \\ \delta & \gamma & \epsilon \end{pmatrix} = \sum_f (-1)^{f-e-\alpha-\delta} (2f+1) W(abcd; ef) \begin{pmatrix} c & a & f \\ \gamma & \alpha & \phi \end{pmatrix} \begin{pmatrix} b & d & f \\ \beta & \delta & -\phi \end{pmatrix}, \quad (\text{C10})$$

thereby obtaining

$$I_{fl}(\hat{\theta}, \hat{\phi}) = |e_q X_0|^2 \frac{(2j+1)}{8\pi} \sum_{J'J''m''} (2n+1)(2J'+1)(2J''+1) P_n(\cos \hat{\theta}) (-1)^{m'+J''+J-J'+q} W(11J'J''; nJ) \\ \times \begin{pmatrix} n & 1 & 1 \\ 0 & -q & q \end{pmatrix} \begin{pmatrix} J & 1 & J' \\ k & 0 & -k \end{pmatrix} \begin{pmatrix} J & 1 & J'' \\ k & 0 & -k \end{pmatrix} \begin{pmatrix} J'' & n & J' \\ -m' & 0 & m' \end{pmatrix} T_{J'jkm''} T_{J''jkm'}. \quad (\text{C11})$$

Straightforward integration over $\hat{\phi}$ then yields the expression (IV.9).

¹O. K. Rice, *J. Chem. Phys.* **1**, 375 (1933).

²R. A. Harris, *J. Chem. Phys.* **39**, 978 (1963).

³R. Zare, *Mol. Photochem.* **4**, 1 (1972).

⁴S. Yang and R. Bersohn, *J. Chem. Phys.* **61**, 4400 (1974).

⁵S. Mukamel and J. Jortner, *J. Chem. Phys.* **61**, 5348 (1974).

⁶R. D. McQuigg and J. G. Calvert, *J. Am. Chem. Soc.* **91**, 1590 (1969).

⁷E. S. Yeung and C. B. Moore, *J. Chem. Phys.* **58**, 3988 (1973).

⁸E. S. Yeung and C. B. Moore, *J. Chem. Phys.* **60**, 2139 (1974).

⁹P. L. Houston and C. B. Moore, *J. Chem. Phys.* **65**, 757 (1976).

¹⁰M. N. R. Ashfold, M. T. MacPherson, and J. P. Simons, *Chem. Phys. Lett.* **55**, 84 (1978).

¹¹M. N. R. Ashfold and J. P. Simons, *Chem. Phys. Lett.* **47**, 65 (1977).

¹²M. N. R. Ashfold and J. P. Simons, *J. Chem. Soc. Faraday Trans. 2* **73**, 858 (1977).

¹³M. N. R. Ashfold and J. P. Simons, *J. Chem. Soc. Faraday Trans. 2* **74**, 280 (1978).

¹⁴M. N. R. Ashfold and J. P. Simons, *J. Chem. Soc. Faraday Trans. 2* **74**, 1263 (1978).

¹⁵M. N. R. Ashfold and J. P. Simons, *J. Chem. Soc. Faraday Trans. 2* **74**, 1965 (1978).

¹⁶A. P. Baranovski and J. R. McDonald, *Chem. Phys. Lett.* **45**, 172 (1977).

¹⁷A. P. Baranovski, R. G. Miller, and J. R. McDonald, *Chem. Phys.* **30**, 119 (1978).

¹⁸M. Asscher, Y. Haas, M. P. Roellig, and P. L. Houston, *J. Chem. Phys.* **72**, 768 (1980).

¹⁹P. J. Dagdigian and R. N. Zare, *J. Chem. Phys.* **61**, 2464 (1974).

²⁰G. P. Smith and R. N. Zare, *J. Chem. Phys.* **64**, 2632 (1976).

²¹P. J. Dagdigian, *Chem. Phys.* **21**, 453 (1977).

²²K. E. Holdy, L. C. Klotz, and K. R. Wilson, *J. Chem. Phys.* **52**, 4588 (1970).

²³M. Shapiro and R. D. Levine, *Chem. Phys. Lett.* **5**, 499 (1970).

²⁴M. J. Berry, *Chem. Phys. Lett.* **27**, 73 (1974).

²⁵M. J. Berry, *Chem. Phys. Lett.* **29**, 329 (1974).

²⁶Y. B. Band and K. F. Freed, *Chem. Phys. Lett.* **28**, 328 (1974).

²⁷Y. B. Band and K. F. Freed, *J. Chem. Phys.* **63**, 3382 (1974).

²⁸K. F. Freed and Y. B. Band, *Excited States* **3**, 109 (1977).

²⁹O. Atabek, J. A. Beswick, R. Lefebvre, S. Mukamel, and J. Jortner, *J. Chem. Phys.* **65**, 4035 (1976).

³⁰U. Halavee and M. Shapiro, *Chem. Phys.* **21**, 105 (1977).

³¹M. Shapiro, *Chem. Phys. Lett.* **46**, 442 (1977).

³²D. Florida and S. A. Rice, *Chem. Phys. Lett.* **33**, 207 (1975).

³³M. D. Morse, K. F. Freed, and Y. B. Band, *Chem. Phys. Lett.* **44**, 125 (1976).

- ³⁴M. D. Morse, K. F. Freed, and Y. B. Band, *J. Chem. Phys.* **70**, 3604 (1979).
- ³⁵M. D. Morse, K. F. Freed, and Y. B. Band, *J. Chem. Phys.* **70**, 3620 (1979).
- ³⁶M. D. Morse, K. F. Freed, and Y. B. Band, *Chem. Phys. Lett.* **67**, 294 (1979).
- ³⁷K. F. Freed and S. H. Lin, *Chem. Phys.* **11**, 409 (1975).
- ³⁸E. Merzbacher, *Quantum Mechanics*, 2nd ed. (Wiley, New York, 1970), p. 61.
- ³⁹C. H. Townes and A. L. Schawlow, *Microwave Spectroscopy* (Dover, New York, 1975), p. 32.
- ⁴⁰Y. B. Band, K. F. Freed, and D. J. Kouri, *J. Chem. Phys.* **74**, 4380 (1981).
- ⁴¹J. T. Hougen and J. K. G. Watson, *Can. J. Phys.* **43**, 298 (1965).
- ⁴²M. E. Rose, *Elementary Theory of Angular Momentum* (Wiley, New York, 1975).
- ⁴³I. S. Gradshteyn and I. M. Ryzhik, *Table of Integrals, Series and Products*, 4th ed. (Academic, New York, 1965).
- ⁴⁴Y. B. Band, M. D. Morse, and K. F. Freed, *J. Chem. Phys.* **68**, 2702 (1978).
- ⁴⁵J. Solomon, *J. Chem. Phys.* **47**, 889 (1967).
- ⁴⁶R. Bersohn and S. H. Lin, *Adv. Chem. Phys.* **16**, 67 (1969).
- ⁴⁷C. Jonah, *J. Chem. Phys.* **55**, 1915 (1971).
- ⁴⁸C. Jonah, P. Chandra, and R. Bersohn, *J. Chem. Phys.* **55**, 1903 (1971).
- ⁴⁹J. Solomon, C. Jonah, P. Chandra, and R. Bersohn, *J. Chem. Phys.* **55**, 1908 (1971).
- ⁵⁰S. C. Yang and R. Bersohn, *J. Chem. Phys.* **61**, 4400 (1974).
- ⁵¹M. Dzvonic, S. Yang, and R. Bersohn, *J. Chem. Phys.* **61**, 4408 (1974).
- ⁵²M. Kawasaki, S. J. Lee, and R. Bersohn, *J. Chem. Phys.* **63**, 809 (1975).
- ⁵³M. Kawasaki, S. J. Lee, and R. Bersohn, *J. Chem. Phys.* **66**, 2647 (1977).
- ⁵⁴G. E. Busch, J. R. Cornelius, R. T. Mahoney, R. I. Morse, D. W. Schlosser, and K. R. Wilson, *Rev. Sci. Instrum.* **41**, 1066 (1970).
- ⁵⁵G. E. Busch and K. R. Wilson, *J. Chem. Phys.* **56**, 3626 (1972).
- ⁵⁶G. E. Busch and K. R. Wilson, *J. Chem. Phys.* **56**, 3638 (1972).
- ⁵⁷J. H. Ling and K. R. Wilson, *J. Chem. Phys.* **63**, 101 (1975).
- ⁵⁸R. W. Diesen, J. Wahr, and S. E. Adler, *J. Phys. Chem.* **55**, 2812 (1971).
- ⁵⁹D. M. Brink and G. R. Satchler, *Angular Momentum*, 2nd ed. (Clarendon, Oxford, 1975).
- ⁶⁰K. F. Freed and J. R. Lombardi, Jr., *J. Chem. Phys.* **45**, 591 (1966).